A Late Devonian actinopterygian suggests high lineage survivorship across the end-Devonian Mass Extinction

Sam Giles[1,2,*], Kara Feilich[3], Rachel Warnock[4], Stephanie E. Pierce[5], Matt Friedman[2,6]

[1]School of Geography Earth and Environmental Sciences, University of Birmingham, Birmingham B15 2TT, UK; [2]Department of Earth Sciences, Natural History Museum, Cromwell Road, London SW7 5BD, UK; [3]Department of Earth and Environmental Sciences, University of Michigan, 1105 N University Ave, Ann Arbor, MI 48109, USA.; [4]GeoZentrum Nordbayern, Friedrich-Alexander-Universität Erlangen-Nürnberg, Loewenichstraße 28, 91054 Erlangen Germany; [5]Museum of Comparative Zoology and Department of Organismic and Evolutionary Biology, Harvard University, 26 Oxford Street, Cambridge, MA 02138, USA; [6]Museum of Paleontology and Department of Earth and Environmental Sciences, University of Michigan, 1105 N University Ave, Ann Arbor, MI 48109, USA.

*Corresponding author: Sam Giles, s.giles.1@bham.ac.uk.

Abstract Many accounts of the early history of actinopterygians (ray-finned fishes) posit that the End Devonian Mass Extinction had a major influence on their evolution. Existing phylogenies suggest this episode could have acted as a bottleneck, paring the early diversity of the group to a handful of survivors. This picture, coupled with increases in taxonomic and morphological diversity in the Carboniferous, contributes to a model of explosive post-extinction radiation. However, most actinopterygians from within a ~20-million-year (Myr) window surrounding the extinction remain poorly known, contributing to uncertainty about the meaning of these patterns. Here, we report an exceptionally preserved fossil from 7 Myr before the extinction that reveals unexpected anatomical features. *Palaeoneiros clackorum* gen. et sp. nov. nests within a clade of post-Devonian species and, in an expanded phylogenetic analysis, draws multiple lineages of Carboniferous actinopterygians into the Devonian. This suggests cryptic but extensive lineage diversification in the latest Devonian, followed by more conspicuous feeding and locomotor structure diversification in the Carboniferous. Our revised model matches more complex patterns of divergence, survival, and diversification around the Devonian-Carboniferous boundary in other vertebrate clades. It also fundamentally recalibrates the onset of diversification early in the history of this major radiation.

Main

The distinction between Devonian and Carboniferous vertebrate faunas has long been apparent[1,2]. Debate on the underlying cause of this faunal turnover focuses on whether it reflects a sudden transition stemming from a mass extinction event (or events) followed by explosive evolutionary recovery[3,4], or a more gradual shift obscured by incomplete or understudied paleontological evidence[5,6]. Taken at face value, the fossil record of actinopterygians (ray-finned fishes) appears to provide strong evidence for the former hypothesis. Actinopterygians persisted at low diversity[3] and abundance[7,8] throughout the Devonian, but assumed their role as the dominant group of aquatic vertebrates in the early Carboniferous[3]. Two important patterns of phenotypic change are associated with this taxonomic shift. First, Carboniferous actinopterygians show a significantly greater repertoire of body and skull shapes than their Devonian predecessors[9], including feeding[10,11] and locomotory[12] innovations. Second, there are indications of body-size reduction in actinopterygians and other vertebrate lineages at this time, interpreted as a protracted 'Lilliput effect'[13].

Unstable phylogenetic relationships and a rudimentary understanding of latest Devonian and earliest Carboniferous actinopterygians complicates interpretation of these patterns. Consensus views on phylogeny indicate only one or two actinopterygian lineages crossed the Devonian-Carboniferous boundary[14-16] (but see[17]), suggesting that prolific diversity in the early Carboniferous arose through an explosive evolutionary radiation seeded by a handful of surviving groups, a mechanism historically proposed for famous examples like placental mammals[18]. Recent analysis suggests an additional Devonian lineage persisted into the early Carboniferous alongside a single radiation containing all Carboniferous and younger taxa[19]. These models contrast with the emerging picture for other vertebrate survivors of the end-Devonian Hangenberg extinction: divergence of multiple lineages in the Late Devonian, followed by substantial ecomorphological radiation in the early Carboniferous. Inadequate taxonomic sampling in early actinopterygian phylogenies hinders meaningful discrimination among these models. Most well-known taxa occur millions of years before[20] or after[15,21,22] the Devonian-Carboniferous boundary. Taxa from deposits more proximate to the extinction[23-26] are rarely included in systematic analyses because of a limited understanding of their anatomy stemming from their small size[25], incomplete preservation[26], or both. However, fossils from the latest Devonian[27] or earliest Carboniferous[19,28] hint at a radically different interpretation of divergences before, survivorship across, and diversification after the end-Devonian extinction.

Here we use micro-computed tomography to provide detailed anatomical information for a new genus and species of actinopterygian from the Late Devonian (middle Famennian; ca. 367 Ma) of the Appalachian Basin of the eastern United States. Previously referred to the problematic genus *Rhadinichthys*[29], it bears an unexpected combination of derived features previously known only in Carboniferous and younger actinopterygians. This taxon prompts a reconsideration of trait evolution and tree topology that together provide evidence for substantial radiation of ray-finned fishes before the end-Devonian mass extinction. This new perspective on ray-finned fish evolution complements evidence in other groups for more complex patterns of evolution through end-Devonian ecological crises[30-35].

Systematic Paleontology

Actinopterygii

Palaeoneiros gen. nov.

Etymology. Greek; *palaeo*, meaning ancient, and *onieros*, the personification of a dream in Greek mythology.

Diagnosis. As for species.

Palaeoneiros clackorum sp. nov.

The Life Science Identifier (LSID) for this publication is: urn:lsid:zoobank.org:pub:E074F1AC-27E2-431C-9AEB-E376C75CF0A4.

Etymology. In honor of Jennifer and Rob Clack, in recognition of their contribution to the fossil record of vertebrates from the Devonian and Carboniferous.

Diagnosis. Actinopterygian characterized by the following combination of characters: ornament on dermal cranial bones comprising broad ridges incised with narrow grooves; dermosphenotic with well-developed posterior ramus; three suborbitals; ramifying tubules of infraorbital canals in jugal; median perforation in aortic canal; two accessory vomers; dermal basipterygoid process; dermohyal unfused to imperforate hyomandibula.

Holotype. MCZ VPF-5114, a nearly complete fish preserved in part and counterpart, missing snout, anterior portion of lower jaw, and caudal fin (Extended Data Figs. 1–2).

Horizon and locality. "Chemung" of Warren, Pennsylvania, USA[29]. The Chemung of earlier workers is a facies rather than formal stratigraphic unit, represented in the Chadakoin and Canadaway formations in western Pennsylvania[36,37]. Only the younger of these, the Chadakoin Formation, is present in the collection locality[36]. The Chadakoin Formation lies within the *Palmatolepis marginifera* Conodont Zone[38,39], Goniatite Zone II-G[39], and Fa2c subdivision of Spore Zone GF[40], indicating a mid-Famennian age, providing a constraint of 367.9-367.2 Ma for MCZ VPF-5114[41]. Other fishes reported from the Chadakoin Formation include arthrodire placoderms, chondrichthyans, lungfishes, and porolepiforms[29,42].

Remarks. Eastman[29] referred MCZ VPF-5114 to the problematic genus *Rhadinichthys*, leaving it in open nomenclature as *Rhadinichthys* sp. Species assigned to *Rhadinichthys* do not form a clade[14], and the holotype of the type species, *R. ornatissimus*, is poorly preserved (National Museum of Scotland NMS G.1878.18.7). There is no evidence linking MCZ VPF-5114 to this taxon to the exclusion of other early actinopterygians. *Palaeoneiros* is small (~55 mm from the tip of the snout to the last of the dorsal ridge scales), but not exceptionally so. Some aspects of its anatomy, including incomplete mineralization of the braincase and palatoquadrate, may be consistent with an immature ontogenetic stage. However, dermal bones are robust with well-developed ornament, and scale cover is complete across the body. Limited ontogenetic data is reported for early actinopterygians, but comparison suggests this individual may be adult or near-adult[43-45].

Results

Skull roof. The skull roof comprises frontals, parietals, supratemporals and intertemporals (Fig. 1A, Extended Data Figs. 3–5). The frontal, which is pierced by the pineal foramen, is the largest bone of the skull roof. It is unclear whether the frontals were tightly joined or fused as a single plate. A notch on the lateral margin of the frontal accommodates the supratemporal. The supraorbital canal, housed on the ventral surface of the frontal and parietal, is fully enclosed anteriorly but unclosed posterior to the level of the pineal foramen. The quadrate parietal bears posterior and middle pit-lines in addition to a short posterior extension of the supraorbital canal. A modest intertemporal lies anterior to the parietal-frontal contract. It carries a short segment of the infraorbital canal along its thickened ventrolateral margin. The lenticular supratemporal is very long, and the infraorbital canal in a ridge along its lateral margin. The lateral margin of the supratemporal abuts the preoperculum, and posterior to this contact a branch of the infraorbital canal extends toward the preopercular canal to form a jugal canal.

Cheek. The cheek comprises a dermosphenotic, jugal, lacrimal, three suborbitals, and preoperculum (Figs. 1A, 2B,C, 3A, Extended Data Figs. 3–5). The dermosphenotic is 'T'-shaped, with long anterior and

posterior limbs and a short ventral limb. The infraorbital canal extends through the ventral limb into the jugal, and a branch in the anterior limb approaches but does not connect with the supraorbital canal of the frontal. Within the jugal, the canal is offset from the orbital margin, and at least 14 branches radiate into its posterior portion. The lacrimal is formed as a tube of bone surrounding the infraorbital canal. Three suborbitals lie between the dorsal limb of the jugal and the anterior margin of the preoperculum. They are arranged in a vertical series, with the middle suborbital smaller than the dorsal and ventral ones. The preoperculum, which bears two pit lines, is boomerang-shaped, with an anterior limb broader than the ventral limb. The angle between these limbs bears a broad overlap area for the maxilla. The preopercular canal extends in a thickened ridge on the inner surface of the bone, near its dorsal margin. The presence of a quadratojugal is uncertain.

Upper jaw and palate. Preserved components of the upper jaw include the maxilla, a putative premaxilla, the quadrate and the dermal palatal bones (Fig. 1A,B, 2A, Extended Data Figs. 3–5).The maxilla is cleaver-shaped with a posteroventral extension and its posterior margin is very thin. A narrow shelf extends along the medial surface of the bone, beginning at the tip of the suborbital limb and continuing to the lower jaw overlap. Ornament on the maxilla comprises a series of broad, flat ridges that are only narrowly separated from each other, resembling a plateau of enamel separated by narrow grooves. Only empty tooth sockets are preserved. Marginal teeth are not visible, but this may represent a limit to scan resolution. A narrow, elongate, tooth-bearing bone medial to the maxilla may represent a displaced premaxilla.

The endoskeletal portion of the palate is largely unmineralized. Only the quadrate is well-ossified, with two prominent condyles. The dermal ossifications of the palate are preserved as separate bones, but divisions between them are not always clear. The ectopterygoid is long and ovoid, with an irregular anterior margin and narrowing to a posteriorly. Dorsally, it is bordered by at least three separately ossified dermatopterygoids, although a gap between two of these suggests four were present in total. Ventral to the entopterygoid, the dermopalatines presumably form a long narrow extension continuous with the ectopterygoid, although no sutures between them are visible. The rectangular entopterygoid lies dorsal to the anterior half of the dermopalatine series.

Two accessory vomers on each side of the skull are closely associated with the parasphenoid. The anterior accessory vomer is approximately twice the length of the posterior one, and tapers slightly anteriorly. It is confined anterior to the basipterygoid process and broadly overlaps the parasphenoid, while the posterior accessory vomer traces the spiracular groove on the ascending process of the parasphenoid.

Lower jaw. The lower jaw is incomplete anteriorly but comprises dermal components of the outer and inner surface and the articular (Fig. 1A,B, 2A, Extended Data Figs. 3–5). The external surface of the lower jaw includes a dentary and at least one postdentary bone; the bone in the posterodorsal portion of the lower jaw is very thin, but the dentary-postdentary suture is visible externally. Ornament on the dentary resembles that of the maxilla. The mandibular canal traverses the ventral margin of the dentary and the posteroventral margin of the postdentary. A single row of seven large conical teeth is present along the dorsal margin of the dentary, plus at least seven empty sockets. No marginal dentition is visible, although this may be an artefact of scan resolution.

The mesial surface of the lower jaw is covered by dermal bone, probably representing the prearticular and coronoids, although divisions between bones are indistinct. This complex defines the mesial margin of the adductor fossa posteriorly. A longitudinal ridge is present on the dorsal surface of these dermal bones. No distinct teeth are visible, but modest crenulation of this ridge suggests that small denticles were present. Three irregularly shaped toothplates are applied to the exposed mesial surface of the prearticular/coronoid complex. Narrow gaps separate individual toothplates, which collectively form a large elliptical composite plate.

Only the articular region of Meckel's cartilage is ossified. It bears concave mesial and lateral facets that match the convex condyles on the quadrate.

Neurocranium and parasphenoid. The braincase is only partially ossified and is floored by a short parasphenoid (Fig. 1D, 2D–F, 3B, Extended Data Figs. 3–4). Mineralization of the neurocranium is largely restricted to the otic and occipital region, comprising a basioccipital plate; dorsal, paired exoccipital ossifications; paired, nodular ossifications anterior to the exoccipitals possibly representing intercalars, and a small ossification posterodorsal to the orbit in the sphenotic region. A well-developed aortic canal, pierced by a prominent midline foramen for the efferent artery, extends the length of the basioccipital ossification. The exoccipitals preserve a single foramen on their lateral surfaces, possibly for a spinoccipital nerve.

The parasphenoid comprises a plank-like anterior corpus and a short posterior extension with a rounded margin. Because of poor endocranial mineralization, it is unclear if it bridged a ventral fissure. In cross-section, the anterior corpus is concave ventrally and convex dorsally. A broad, rounded ridge extends along the dorsal midline of the anterior half of the corpus. A denticulated ridge on the ventral surface of the corpus was exposed between the accessory vomers. Three major structures are present near the junction between the anterior corpus and posterior extension of the parasphenoid: a prominent midline buccohypophysial foramen, modest dermal basipterygoid processes, and long ascending processes. Pronounced spiracular grooves extend along the lateral surfaces of the ascending processes. Deep notches mark the posterior intersection of the ascending processes and the body of the parasphenoid, and a parabasal canal is present.

Hyoid arch and associated dermal bones. Endoskeletal ossifications of the hyoid arch include the hyomandibula and ceratohyal, both of which are incompletely mineralized (Fig. 1D, 2F,G, 3C, Extended Data Figs. 3–4). These are joined by a large dermohyal. The imperforate hyomandibula has a distinct elbow marking the junction of its dorsal and ventral limbs, and lacks an opercular process. A groove on the dorsomedial surface of the upper limb marks the course of the hyomandibular branch of the facial nerve. Mineralization of the hyomandibula is incomplete proximally and distally. The plate-like ceratohyal lacks a medial constriction and bears a lateral groove for the afferent hyoid artery. The proximal and distal ends of the bone are unmineralized. The triangular dermohyal is longer than the preserved dorsal shank of the hyomandibula, and the two are unfused.

Branchial arches. Mineralization of the gill skeleton is generally poor throughout (Fig. 1D, 2F, Extended Data Figs. 3–4,6). The gill skeleton has four rod-like ceratobranchials bearing a longitudinal ventral groove, with a poorly mineralized and narrow fifth arch visible in the scan but beyond the limit of segmentation. Paired bones representing hypobranchial 1 lie at the anterior of the gill skeleton, displaced from life position. Hypobranchial 1 is one third the length of ceratobranchial 1, and has a ventral process at its proximal end. The basibranchial is largely unossified, but a small segment bearing paired swellings is preserved anterior to the second ceratobranchials. Two epibranchials are mineralized on each side of the skull. Each bears a dorsal longitudinal groove and an uncinate process. A single pharyngobranchial is preserved on each side of the specimen, in articulation with the basioccipital.

Operculogular series. The operculogular series comprises an operculum, subopercular, and branchiostegals (Fig 1A, Extended Data Figs. 3–4). The rhombic operculum has a long diagonal axis and small prong at its anterior corner. Ridges ornament the external surface of the bone. The quadrangular subopercular is half the size of the operculum. Around 13 splint-shaped branchiostegals are preserved, the most posterior of which is the deepest. As the anteriormost branchiostegals are exposed, it is not possible to determine their exact number or identify any gular plates.

Pectoral girdle and fin. The dermal shoulder girdle includes extrascapulars, a posttemporal, presupracleithrum, supracleithrum, cleithrum, and clavicle (Fig. 1A,C,D, Extended Data Figs. 3–4,7). As only one half of the skull roof is preserved, the exact number of extrascapulars is unknown, but it seems

likely that only one bone was present per side. There is no trace of a medial branch of the lateral line canal. The leaf-shaped posttemporal makes a broad contact with the extrascapular(s), and overlaps the presupracleithrum and supracleithrum. A pronounced groove for the lateral line is visible on the supracleithrum. The cleithrum is broad, with laterally directed and medially directed faces separated by a medial ridge. The clavicles are strongly curved, with a long, narrow anterodorsal extension. Clavicles and cleithra are ornamented with long ridges. The interclavicle is elongate and arrow-shaped, and only a narrow ridge on its ventral surface would have been exposed between the clavicles. At least three proximate lepidotrichs are fused together at the leading edge of the fin, although they do not appear to embrace the propterygium. The remaining lepidotrichs are evenly segmented and bifurcate distally. Fringing fulcra are absent.

The endoskeletal shoulder girdle and radials are well ossified (Fig. 1C, Extended Data Figs. 3–4,7). The scapulocoracoid is present as several separate ossifications. The largest portion is a curved, horizontal ossification, the lateral face of which abuts the cleithrum and the posterior face of which contacts the propterygium. The remaining radials were presumably supported by a cartilaginous extension. Three flat, curved plates, each smaller and narrower than the horizontal ossification, comprise the remainder of the scapulocoracoid, but do not appear to be in life position. Three stout, rod-like radials are present between the metapterygium and propterygium. The propterygium is complex in shape, more than twice the size of any other radial and pierced by the propterygial canal. The metapterygium is longer than the remaining radials and supports one preaxial radial.

Little of the remaining fins can be described. Basal scutes are absent. The anal fin bears fringing fulcra, and pelvic fins are present.

Scales. The scales are rhombic, with an internal ridge and peg-and-socket articulation (Extended Data Figs. 2–4). Ornament comprises broad flat ridges of enamel incised with roughly parallel narrow grooves.

Discussion

Anatomical comparisons and phylogenetic placement. Our data reveal internal anatomy unanticipated in a Devonian actinopterygian (Fig. 2A-C). Most prominent are a midline perforation in the aortic canal and dermal basipterygoid processes, previously known only in post-Devonian taxa[22,46-49]. This is joined by features such as suborbitals and multiple rami of the infraorbital canal in the jugal, features known only in one or two Devonian species[50-52] (Fig. 2D-F) but overwhelmingly present in younger taxa (Fig. 2H-J). While there are some indications that this specimen may not be fully adult, comparison with development in extant species indicates that the features that ally it with Carboniferous actinopterygians are not transient juvenile features[53,54]. The presence of this character suite in a Devonian actinopterygian has significant implications for the timing of these anatomical changes.

This qualitative assessment is corroborated by formal phylogenetic analysis of a published matrix[55] expanded to incorporate additional Famennian and Tournaisian actinopterygians. Our parsimony (Extended Data Fig. 8) and Bayesian analyses (Extended Data Fig. 9) recover *Palaeoneiros* as a stem actinopterygian in an immediate clade with two Mississippian taxa. In common with previous analyses[16,55], resolution is poor across the Bayesian tree. In our parsimony analysis, *Palaeoneiros* and its sister taxa are recovered in a broader clade of Carboniferous–Triassic and younger ray-finned fishes. The placement of *Palaeoneiros* as nested within a Carboniferous radiation is supported by characters relating to the dermal and endoskeleton (Dataset S5).

We also recover multiple clades containing both Devonian and stratigraphically younger forms. This contrasts with the majority of recent phylogenetic hypotheses, which generally recover all post-Devonian taxa in just one[16,55] or two[14,15,20,56] clades; earlier analyses suggesting more substantial diversification outside of the actinopterygian crown [17,57] are likely biased by methodological and sampling issues[58]. *Palaeoneiros* establishes that key anatomical features previously thought restricted to Carboniferous and

younger taxa arose in the Devonian, and the nested phylogenetic position of *Palaeoneiros* and other Late Devonian taxa provides explicit support for the hypothesis that numerous actinopterygian lineages crossed the end-Devonian boundary.

Models of early actinopterygian diversification. Timing of divergences among early actinopterygians in past studies is either taken at face-value from the fossil record[3,13] or depicted graphically in trees[19,59,60] timescaled using naïve *a posteriori* approaches[61]. Prevailing hypotheses using these approaches posit that just one or two lineages crossed the end-Devonian boundary, with explosive diversification occurring in the early Carboniferous (Fig. 4: inset). Even without formal analysis of divergence times, our placement of *Palaeoneiros* instead supports another model: extensive lineage diversification in the Late Devonian that led directly to the post-extinction radiation (Fig. 4: inset). A fossil birth-death analysis[62] provides a more explicit timescale for early actinopterygian evolution (Fig. 4; Extended Data Fig. 10; Dataset S4), and places the origin of crown actinopterygians in the Late Devonian or earliest Carboniferous (mean: 364.4 Myr; 95% highest posterior density: 379.1 Myr–351.6 Myr). The maximum clade credibility tree suggests that at least ten lineages—an order of magnitude more than inferred by most recent analyses[16,55], and representing high survivorship relative to standing diversity—persisted into the Carboniferous, indicating substantial and hitherto cryptic diversification before the end-Devonian extinction.

Body size represents an important correlate of many aspects of life history and ecology, with many questions centering on impacts of body size during intervals of biotic crisis. Across all marine groups, selectivity on body size is more conspicuous during mass extinctions and their recovery intervals[63]. Decreases of mean body size associated with the Devonian-Carboniferous boundary have previously been reported in many vertebrate clades, including actinopterygians[13]. Our dataset provides a phylogenetically informed assessment of this pattern. While we find a general decrease in body size from the latest Devonian into the early Carboniferous, there is no strong inflection close to the boundary itself (Fig. 5C), and interrogation of size distribution in boundary-crossing lineages suggests that most were mid-sized (Fig. 5B). While *Palaeoneiros* is small, it is comfortably within the size range of other mature Devonian-Carboniferous actinopterygians (Fig. 5A). More densely sampled phylogenetic hypotheses that incorporate taxa currently excluded from many analyses[60] will be necessary for assessing impacts of the Devonian-Carboniferous extinction on the trajectory of body-size evolution in ray-finned fishes, as well as analyses on rates of diversification.

Importantly, the features that nest *Palaeoneiros* and some other Late Devonian taxa within clades composed mostly of younger taxa do not relate to the substantial mandibular and locomotor innovations interpreted as evidence of increased ecological diversity among Carboniferous taxa[9-11,28]. Thus, the initial diversification of actinopterygians appears to show decoupling of cladogenetic events, which took place prior to the end-Devonian extinction, from subsequent ecomorphological and trophic divergence, which took place in the early Carboniferous. Such offsets between lineage divergence and phenotypic diversification are a common feature of vertebrate evolution[64,65]. A similar pattern also seems to characterize the radiation of placental mammals[66,67]. Evidence suggests this might be a common evolutionary trajectory for vertebrate lineages across the Devonian-Carboniferous boundary, with both tetrapods and lungfishes showing substantial lineage diversification before, and morphological divergence after, the extinction[30-35].

Methods

CT scanning. MCZ (Harvard Museum of Comparative Zoology) VPF-5114 was scanned on a Nikon XT 225 ST micro CT scanner at the CTEES facility, Department of Earth and Environmental Sciences, University of Michigan. Details of the scan: voltage = 130 kV; current = 115 μA; exposure = 4 s; frames per projection = 2; projections = 3141; filter = 1 mm Cu. After scanning, data were segmented in Mimics

(http://biomedical.materialise.com/mimics; Materialise, Leuven, Belgium). Surface meshes were then exported into and imaged in Blender (http://blender. org; Stitching Blender Foundation, Amsterdam, the Netherlands).

Phylogenetic analysis. Analyses were performed in TNT v1.5[68] and MrBayes v.3.2.6[69] using a dataset modified from Latimer & Giles[55] and Figueroa et al.[70] with the addition of ten taxa, giving a total of 121 taxa and 292 characters. Full details are given in the Supplementary Information. An equally weighted parsimony analysis was conducted in TNT using the following settings: hold 200000; xmult=level10; bbreak=fillonly. The outgroup was set as *Dicksonoteus arcticus*, and the following topology constraint was applied: [*Dicksonosteus* [*Entelognathus* [*Acanthodes*, *Cladodoides*, *Ozarcus*][ingroup]]]. Bremer decay values were calculated in TNT, and an agreement subtree was calculated in PAUP* 4.0a169[71]. We conducted a Bayesian analysis with no stratigraphic information and identical constraints on outgroup taxa, discarding the first third of the run as burnin. To infer the timescale of early actinopterygian diversification, we also conducted an additional Bayesian analysis under the fossil-birth-death (FBD) model and an independent gamma rate (IRG) relaxed clock model. Taxa were assigned uniform age priors matching the duration of the shortest temporal interval to which they could be assigned (e.g., conodont or ammonoid zones for many Devonian-Carboniferous taxa). We used a uniform prior on the root age *U*(425, 458.18) with the upper bound informed by the early record of ostracoderms. In the absence of meaningful prior estimates of key parameters like preservation, extinction, and speciation rates, we adopted uninformative priors suggested by Matzke & Wright[72]. In addition to constraints among non-osteichthyans, we applied a topological constraint for osteichthyan interrelationships matching the strict consensus from parsimony analyses. Analyses were run for a total of 6,000,000 generations, with two chains.

Trait analysis. Many early actinopterygians are known from incomplete remains, or from articulated but distorted specimens, so we selected mandibular length as a measure of size. Mandibles are taphonomically robust, and easily measured even in disrupted specimens. In order to interrogate patterns of body size evolution, we began with a list of taxa drawn from our phylogenetic analysis and excluded non-actinopterygians, Triassic and younger taxa, and taxa in which the lower jaw length cannot be reliably measured. This left a total of 20 taxa that could be measured based on direct observation of 138 fossil specimens in the Natural History Museum London (specimens prefixed with NHMUK), the National Museums of Scotland (specimens prefixed with NMS and G), the Harvard Museum of Comparative Zoology (specimens prefixed with MCZ), Manchester Museum (specimens prefixed with W), and the Cleveland Museum of Natural History (CMNH). These were combined with measurements for taxa derived from the literature where necessary. The resulting dataset comprised 55 specimens encompassing 20 taxa, including one juvenile (*Melanecta anneae* from ref Coates 1998). Comparison of the natural logarithms of jaw length and total length in this subset of specimens shows a strong correlation between the two measures of size (r = 0.93). In order to estimate trait values among lineages at specific times, we drew on an approach designed to graphically depict changes in continuous traits along branches within a phylogeny[73]. This method, which draws on functions in the R package phytools[74], estimates states for a trait at internal nodes by using the contrasts algorithm of Felsenstein[75]. Trait values at specific points along internal branches were then estimated via interpolation as described by Revell [73]. To summarize patterns over time, we estimated median size at 1-million-year intervals for a 50-million-year time period spanning the Devonian-Carboniferous boundary for a sample of 50 trees drawn from the posterior sample of our FBD analysis. We also pooled the inferred sizes of lineages at this boundary across these 50 trees in order to show patterns in body size distribution beyond central tendency.

Data availability

The specimen described in this study is reposited in the collections of the. Harvard Museum of Comparative Zoology. The CT raw projection series, reconstructed .TIFF stack, and .OBJ file of all segmented 3D objects are available on Morphosource.org (https://www.morphosource.org/concern/biological_specimens/000417029). The Mimics file can be downloaded by contacting the Department of Vertebrate Paleontology at the Museum of Comparative Zoology, Harvard. All other data associated with this paper are included in Supplementary Data.

This work and associated nomenclatural acts are registered in ZooBank. ZooBank LSIDs are accessible at the URL generated by appending the LSID to http://zoobank.org.

Code availability

The code necessary for performing the trait analyses is included in Supplementary Data.

Acknowledgments

We thank the Harvard Museum of Comparative Zoology for specimen access and especially Jessica Cundiff for organizing the loan of material that formed the basis of this study. We also thank Emma Bernard, David Gelsthorpe, Zerina Johanson, Lindsay Loughtman, Paul Shephard and Stig Walsh for facilitating access to comparative collections; Graeme Lloyd for helpful discussions; and Christina Byrd for assistance with data archiving. SG was supported by a Royal Society Dorothy Hodgkin Research Fellowship (DH160098). This research was also supported by joint funding from the National Science Foundation and National Environment Research Council to MF (NSF-GEO 2219007), SG and SEP (NSF GEO-2219069). This study includes data produced in the CTEES facility at University of Michigan, supported by the Department of Earth and Environmental Sciences and College of Literature, Science, and the Arts.

Author Contributions: MF and SEP designed research; SG, MF, KF and RW performed research and analysed data; SG and MF wrote the paper and designed figures; all authors edited text.

Competing Interest Statement: The authors declare no competing interests.

Figure Legends

Figure 1. Anatomy of *Palaeoneiros clackorum* MCZ VPF-5114. Renders of (A) right lateral view of specimen; (B) medial view of right upper and lower jaws; (C) medial view of left shoulder girdle and pectoral fin, and (D) left lateral view of gill skeleton, hyoid arch and braincase. Colour coding of skeleton: blue, cheek and jaw; purple, skull roof and sclerotic ossicle; pink, braincase; dark green, hyomandibula; light green, operculogular system; turquoise, shoulder girdle; yellow, gill skeleton. Scale bar in (A): 10 mm, in (B)-(D): 5 mm. Abbreviations: ang, angular; art, articular; asp, ascending process of parasphenoid; av, accessory vomer; br, branchiostegal; cb, ceratobranchial; chy, ceratohyal; clav, clavicle; clth, cleithrum; dent, dentary; dmpt, dermatopterygoid; dsph, dermosphenotic; eb, epibranchial; ecpt, ectopterygoid and dermopalatines; enpt, entopterygoid; exo, exoccipital; hmd, hyomandibula; ?ic, possible intercalar; icl, interclavicle; it, intertemporal; jug, jugal; lep, lepidotrichia; ll, lateral line; mx, maxilla; op, operculum; part, prearticular and coronoid; ?pmx, possible premaxilla; psp, parasphenoid; qu, quadrate; rad, radials; sc, scale; scl, sclerotic ossicle; scpc, scapulocoracoid; sop, suboperculum; sorb, suborbitals; sph, sphenotic ossification; st, supratemporal; t, teeth; tp, toothplate; unc, uncinate process. Renders copyright President and Fellows of Harvard College.

Figure 2. Internal and external anatomy of *Palaeoneiros clackorum* MCZ VPF-5114. Renders of (A) cheek and dentary in right lateral view; (B) orbit in right lateral view, and (C) with jugal and temporal bones removed; (D) braincase in right lateral and (E) ventral view; (F) hyoid arch, braincase and gill skeleton in right lateral view; (G) hyoid arch in right lateral view. Scale bar in (A), (D)-(G): 5mm, in (B)-(C): 2mm. Abbreviations: ang, angular; ahy, afferent hyoid artery; aoc, aortic canal; asp, ascending process of the parasphenoid; av, accessory vomer; bb, basibranchial; bhc, buccohypophysial canal; boc, basioccipital; cb, ceratobranchial; chy, ceratohyal; dent, dentary; dhy, dermohyal; d.bpt, dermal basipterygoid process; dsph, dermosphenotic; eb, epibranchial; epi.a, foramen for epibranchial artery; exo, exoccipital; hb, hyobranchial; hmd, hyomandibula; ?ic, possible intercalar; it, intertemporal; ioc, infraorbital canal; jug, jugal; la, lacrimal; mx, maxilla; na, nasal; psp, parasphenoid; ram, ramifying tubules of infraorbital canal; scl, sclerotic ossicle; sorb, suborbitals; sph, sphenotic ossification; spig; spiracular groove; st, supratemporal. Renders copyright President and Fellows of Harvard College.

Figure 3. Comparative anatomy of *Palaeoneiros clackorum* with Devonian and Carboniferous actinopterygians. Renders of *Palaeoneiros clackorum* showing (A) cheek in right lateral view, (B) braincase in ventral view, and (C) hyomandibula in right lateral view. Interpretive drawings of *Mimipiscis* showing (D) cheek in right lateral view and (E) braincase in ventral view. Interpretive drawing of (F) *Moythomasia durgaringa* showing hyomandibula in right lateral view. Interpretive drawings of (G) *Cosmoptychius striatus* showing cheek in right lateral view, (H) *Lawrenciella schaefferi* showing braincase in ventral view, and (I) an indeterminate Kasimovian actinopterygian showing hyomandibula in right lateral view; dermohyal nufused and thus not preserved. Path of sensory canals shown in red. Parts of the braincase are masked out in *Mimipiscis* and *Lawrenciella* to facilitate comparison with of *Palaeoneiros*. (D)-(F) redrawn from Gardiner [20], (G) redrawn from Gardiner [76], (H) redrawn from Hamel and Poplin [47], and (I) redrawn from Poplin [22]. Not to scale. Colour of boxes represents geological time period (orange: Devonian; cyan: Carboniferous). Abbreviations: aoc, aortic canal; asp, ascending process of parasphenoid; bhc, buccohypophysial canal; d.bpt, dermal basipterygoid process; dhy, dermohyal; e.bpt, endoskeletal basipterygoid process; epi.a, epibranchial artery; hmc, hyomandibular canal; hmd, hyomandibula; ju, jugal; opc, opercular process; ram, ramifying tubules of infraorbital sensory canal; sorb, suborbitals. Renders copyright President and Fellows of Harvard College.

Figure 4. Hypotheses of early actinopterygian diversification and timescaled phylogenetic tree. Inset: alternative hypotheses of actinopterygian survivorship, where a single lineage[16] or two lineages[19] cross the extinction boundary, with diversification happening in the earliest Carboniferous, or cryptic diversification happening in the latest Devonian, with many lineages crossing the extinction boundary. Main panel: fossil birth-death analysis showing the impact of the inclusion of *Palaeoneiros* and other Famennian/Tournaisian taxa on lineage survivorship across the end-Devonian Mass Extinction. Crown group clades collapsed for clarity, with arrows indicating they continue to the present day; tip position for each branch corresponds to the estimated mean age of taxon sampled; blue bars associated with nodes indicate 95% highest posterior density for age estimates. Full tree given in Extended Data Fig. 10. Position of end-Devonian Mass Extinction marked by red vertical line.

Figure 5. Patterns in early ray-finned fish size around the Devonian-Carboniferous boundary. (A) Specimen-level relationship of jaw size and standard length (natural logarithms of these linear measures shown throughout figure). Jaw size of *Palaeoneiros* indicated by vertical dotted line. Hollow circle indicates juvenile. Colour of points represents geological time period (orange: Devonian; cyan: Carboniferous). (B) Size distribution of boundary-crossing lineages estimated from a sample of 50 trees drawn from the posterior distribution of a Bayesian phylogenetic analysis using the fossilized birth-death prior. (C) Median size estimated at 1 Myr intervals (values inferred along branches plus any coincident tips) during the Late Devonian and early-mid Carboniferous. Black line indicates mean of 50 trajectories (individual grey lines) based on 50 trees drawn from the posterior sample. Position of end-Devonian Mass Extinction marked by red vertical line. Statistical support value in (A) represents Spearman's rank correlation.

References

1 Woodward, A. S. *Catalogue of the Fossil Fishes in the British Museum (Natural History). Part II. Containing the Elasmobranchii (Acanthodii), Holocephali, Ichthyodorulites, Ostracodermi, Dipnoi, and Teleostomi (Crossopterygii and Chondrostean Actinopterygii)*. (Trustees of the British Museum (Natural History), 1881).

2 Woodward, A. S. *Catalogue of the Fossil Fishes in the British Museum (Natural History). Part III. Containing the Actinopterygian Teleostomi of the Orders Chondrostei (Concluded), Protospondyli, Aethospondyli, and Isospondyli (In Part)*. 544 (Trustees of the British Museum, 1895).

3 Sallan, L. C. & Coates, M. I. End-Devonian extinction and a bottleneck in the early evolution of modern jawed vertebrates. *Proceedings of the National Academy of Sciences of the USA* **107**, 10131-10135 (2010).

4 Smithson, T. R., Richards, K. R. & Clack, J. A. Lungfish diversity in Romer's Gap: reaction to the end-Devonian extinction. *Palaeontology* **59**, 29-44 (2016).

5 Anderson, J. S., Smithson, T. R., Masksy, C. F., Meyer, T. & Clack, J. A. A diverse tetrapod fauna from the base of 'Romer's Gap'. *PLoS ONE* **10**, e0125446 (2015).

6 Smithson, T. R., Wood, S. P., Marshall, J. E. A. & Clack, J. A. Earliest Carboniferous tetrapod and arthropod faunas populate Romer's Gap. *Proceedings of the National Academy of Sciences of the USA* **109**, 4532-4537 (2012).

7 Long, J. A. & Trinajstic, K. The Late Devonian Gogo Formation Lägerstatte of Western Australia: Exceptional Early Vertebrate Preservation and Diversity. *Annual Reivew of Earth and Planetary Sciences* **38**, 255-279 (2010).

8 Trewin, N. H. Palaeoecology and sedimentology of the Achanarras fish bed of the Middle Old Red Sandstone, Scotland. *Transactions of the Royal Society of Edinburgh: Earth Sciences* **77**, 21-46 (1986).
9 Sallan, L. C. & Friedman, M. Heads or tails: staged diversification in vertebrate evolutionary radiations. *Proceedings of the Royal Society B* **279**, 2025-2032 (2012).
10 Friedman, M., Pierce, S. E., Coates, M. I. & Giles, S. Feeding structures in the ray-finned fish *Eurynotus crenatus* (Actinopterygii: Eurynotiformes): implications for trophic diversification among Carboniferous actinopterygians. *Earth and Environmental Science Transactions of the Royal Society of Edinburgh* **109**, 33-47 (2019).
11 Sallan, L. C. & Coates, M. I. Styracopterid (Actinopterygii) ontogeny and the multiple origins of post-Hangenberg deep-bodied fishes. *Zoological Journal of the Linnean Society* **169**, 156-199 (2013).
12 Sallan, L. Tetrapod-like axial regionalization in an early ray-finned fish. *Proceedings of the Royal Society B* **279**, 3264-3271 (2012).
13 Sallan, L. C. & Galimberti, A. K. Body-size reduction in vertebrates following the end-Devonian mass extinction. *Science* **350**, 812-815 (2015).
14 Gardiner, B. G. & Schaeffer, B. Interrelationships of lower actinopterygian fishes. *Zoological Journal of the Linnean Society* **97**, 135-187 (1989).
15 Coates, M. I. Endocranial preservation of a Carboniferous actinopterygian from Lancashire, UK, and the interrelationships of primitive actinopterygians. *Philosophical Transactions of the Royal Society B* **354**, 435-462 (1999).
16 Giles, S., Xu, G.-H., Near, T. J. & Friedman, M. Early members of a 'living fossil' lineage imply later origin of modern ray-finned fishes. *Nature* **549**, 265-268 (2017).
17 Cloutier, R. & Arraita, G. in *Recent Advances in the Origin and Early Radiation of Vertebrates* (eds G. Arratia, M. V. H. Wilson, & R. Cloutier) 217-270 (Verlag Dr. Friedrich Pfeil, 2004).
18 O'Leary, M. A. *et al.* The placental mammal ancestor and the post-K-Pg radiation of placentals. *Science* **339**, 662-667 (2013).
19 Wilson, C. D., Pardo, J. D. & Anderson, J. S. A primtive actinopterygian braincase from the Tournaisian of Nova Scotia. *Royal Society Open Science* **5**, 171727 (2018).
20 Gardiner, B. G. The relationships of the palaeoniscid fishes, a review based on new species of *Mimia* and *Moythomasia* from the Upper Devonian of Western Australia. *Bulletin of the British Museum (Natural History) Geology* **37**, 173-428 (1984).
21 Coates, M. I. Actinoptergians from the Namurian of Bearsden, Scotland, with comments on early actinopterygian neurocrania. *Zoological Journal of the Linnean Society* **122**, 27-59 (1998).
22 Poplin, C. *Étude de quelques paléoniscidés pennsylvaniens du Kansas*. 151 (Éditions du CNRS, 1974).
23 Dunkle, D. H. Preliminary description of a paleoniscoid fish from the Upper Devonian of Ohio. *Scientific Publications of the Cleveland Museum of Natural History, New Series* **3**, 1-16 (1964).
24 Friedman, M. & Blom, H. A new actinopterygian from the Famennian of East Greenland and the interrelationships of Devonian ray-finned fishes. *Journal of Paleontology*, 1186-1204 (2006).
25 Daeschler, E. B. An early actinopterygian fish from the Catskill Formation (Late Devonian, Famennian) in Pennsylvania, U.S.A. *Proceedings of the Academy of Natural Sciences of Philadelphia* **150**, 181-192 (2000).
26 Prokofiev, A. M. First finding of an articulated actinopterygian skeleton from the Upper Devonian of Siberia and a reappraisal of the family Moythomasiidae Kazantseva, 1971 (Osteichthyes). *Paleontological Research* **6**, 321-327 (2002).

27 Janvier, P., Lethiers, F., Monod, O. & Balkas, Ö. Discovery of a vertebrate fauna at the Devonian-Carboniferous boundary in SE Turkey (Hakkari Province). *Journal of Petroleum Geology* **7**, 147-168 (1984).
28 Wilson, C. D., Mansky, C. F. & Anderson, J. S. A platysomid occurrence from the Tournaisian of Nova Scotia. *Scientific Reports* **11.1**, 1-12 (2021).
29 Eastman, C. R. *Devonic Fishes of the New York Formations*. 235 (New York State Education Dept., 1907).
30 Challands, T. J. *et al.* A lungfish survivor of the end-Devonian extinction and an Early Carboniferous dipnoan radiation. *Journal of Systematic Palaeontology*, doi:10.1080/14772019.2019.1572234 (2019).
31 Clack, J. A., Challands, T. J., Smithson, T. R. & Smithson, K. Z. Newly recognized Famennian lungfishes from East Greenland reveal tooth plate diversity and blur the Devonian-Carboniferous boundary. *Papers in Palaeontology* **5**, 261-279 (2019).
32 Anderson, J. S., Smithson, T., Mansky, C. F., Meyer, T. & Clack, J. A. A diverse tetrapod fauna at the base of 'Romer's Gap'. *PLoS ONE* **10**, e102446 (2015).
33 Daeschler, E. B., Clack, J. A. & Shubin, N. H. Late Devonian tetrapod remains from Red Hill, Pennsylvania, USA: how much diversity? *Acta Zoologica* **90**, 306-317 (2009).
34 Ahlberg, P. E. & Clack, J. A. The smallest known Devonian tetrapod shows unexpectedly derived features. *Royal Society Open Science* **7**, 192117 (2020).
35 Pardo, J. D., Szostakiwskyj, M., Ahlberg, P. E. & Anderson, J. S. Hidden morphological diversity among early tetrapods. *Nature* **546**, 642-645 (2017).
36 (ed A. A. Socolow) (Commonwealth of Pennsylvania, Department of Environmental Resources, 1980).
37 Startenaer, P. *Jacoburbirostrum*, a new middle Famennian rhynchonellid (brachiopod) genus from southwestern New York State. *Bulletin of Geosciences* **89**, 607-616 (2014).
38 Kirchgasser, W. T. in *Recognition of Devonian sereis and stage boundaries in geological areas* Vol. 225 *Courier Forschungsinstitut Senckenberg* (ed P. Bultynck) 271-284 (2000).
39 House, M. R. & Kirchgasser, W. T. Late Devonian goniatites (Cephalopoda, Ammonoidea) from New York State. *Bulletins of American Paleontology* **374**, 1-285 (2008).
40 Clendening, J., A., Eames, L. E. & Wood, G. D. *Retusotriletes phillipsii* n. sp., a potential Upper Devonian guide palynomorph. *Palynology* **4**, 15-21 (1980).
41 Becker, R. T., Marshall, J. E. A. & Da Silva, A.-C. in *Geologic Time Scale 2020* (eds F. M. Gradstein, J. G. Ogg, M. D. Schmitz, & G. M. Ogg) 733-810 (Elsevier, 2020).
42 Yeager, K. M. Fossil fishes (Arthrodira and Acanthodida) from the Upper Devonian Chadokoin Formation of Erie County, Pennsylvania. *Ohio Journal of Science* **96**, 52-56 (1996).
43 Lowney, K. A. *Certain Bear Gulch (Namurian A, Montana) Actinopterygii (Osteichthyes), and a re-evaluation of the evolution of the Paleozoic actinopterygians* PhD thesis, New York University, (1980).
44 Coates, M. I. New actinopterygian fish from the Namurian Manse Burn Formation of Bearsden, Scotland. *Palaeontology* **36**, 123-146 (1993).
45 Schultze, H.-P. & Bardack, D. Diversity and size changes in palaeonisciform fishes (Actinopterygii, Pisces) from the Pennsylvanian Mazon Creek fauna, Illinois, U.S.A. *Journal of Vertebrate Paleontology* **7**, 1-23 (1984).
46 Rayner, D. H. n the Cranial Structure of an Early Palæoniscid, Kentuckia, gen. nov. . *Transactions of the Royal Society of Edinburgh* **62**, 53-83 (1952).

47 Hamel, M. H. & Poplin, C. The braincase anatomy of *Lawrenciella schaefferi*, actinopterygian from the Upper Carboniferous of Kansas (USA). *Journal of Vertebrate Paleontology* **28**, 989-1006 (2008).
48 Schaeffer, B. & Dalquest, W. W. A palaeonisciform braincase from the Permian of Texas, with comments on cranial fissures and the posterior myodome. *American Museum Novitates* **2658**, 1-15 (1978).
49 Nielsen, E. Studies on Triassic fishes I. *Meddelelser om Grønland* **138**, 1-394 (1942).
50 Jessen, H. *Moythomasia nitida* Gross und *M*. cf. *striata* Gross, Devonische Palaeonisciden aus dem oberen Plattenkalk der Bergisch-Gladbach-Paffrather Mulde (Rheinisches Schiefergebirge). *Palaeontographica Abteilung A* **128**, 87-114 (1968).
51 Choo, B. A new species of the Devonian actinopterygian *Moythomasia* from Bergisch Gladbach, Germany, and fresh observations on *M. durgaringa* from the Gogo Formation of Western Australia. *Journal of Vertebrate Paleontology* **35**, e952817 (2015).
52 Taverne, L. Osorioichthys marginis, "Paléonisciforme" du Famennien de Belgique, et la phylogénie des Actinoptérygiens dévoniens (Pisces). *Bulletin de l'Institut Royal des Sciences Naturelles de Belgique, Sciences de la Terre* **67**, 57-78 (1997).
53 Moy-Thomas, J. A. Memoirs: notes on the development of the chondrocranium in *Polypterus senegalus*. *Journal of Cell Science* **(2) 76**, 209-229 (1933).
54 Daget, J., Bauchot, M. L., Bauchot, R. & Arnoult, J. Développement du chondrocrâne et des arcs aortiques chez Polypterus senegalus Cuvier. *Acta Zoologica* **45**, 201-244 (1964).
55 Latimer, A. E. & Giles, S. A giant dapediid from the Late Triassic of Switzerland and insights into neopterygian phylogeny. *Royal Society Open Science* **5**, 180497 (2018).
56 Gardiner, B. G., Schaeffer, B. & Masserie, J. A. A review of the lower actinopterygian phylogeny. *Zoological Journal of the Linnean Society* **144**, 511-525 (2005).
57 Mickle, K. E., Lund, R. & Grogan, E. Three new palaeoniscoid fishes from the Bear Gulch Limestone (Serpukhovian, Mississippian) of Montana (USA) and the relationships of lower actinopterygians. *Geodiversitas* **31**, 623-668 (2009).
58 Sallan, L. C. Major issues in the origin of ray-finned fish (Actinopterygii) biodiversity. *Biological Reviews* **89**, 950-971 (2014).
59 Friedman, M. The early evolution of ray-finned fishes. *Palaeontology* **58**, 213-228 (2015).
60 Henderson, S., Dunne, E. M. & Giles, S. The early diversification of ray-finned fishes (Actinopterygii): hypotheses, challenges, and future prospects. *EarthArXiv*, doi:https://doi.org/10.31223/X58D1D (2022).
61 Bapst, D. W. & Hopkins, M. J. Comparing cal3 and other a posteriori time-scaling approach in a case study with the pterocephaliid trilobites. *Paleobiology* **43**, 49-67 (2017).
62 Heath, T. A., Huelsenbeck, J. P. & Stadler, T. The fossilized birth-death process for coherent calibration of divergence-time estimates. *Proceedings of the National Academy of Sciences of the USA* **111**, E2957-E2966 (2014).
63 Monarrez, P. M., Heim, N. A. & Payne, J. L. Mass extinctions alter exinction and origination dynamics with respect to body size. *Proceedings of the Royal Society B* **288**, 20211681 (2021).
64 Cantalapiedra, J. L., Prado, J. L., Hernández-Fernández, M. & Alberdi, M. T. Decoupled ecomorphological evolution and diversification in Neogene-Quaternary horses. *Science* **355** (2017).
65 Simões, T., Vernygora, O., Caldwell, M. W. & Pierce, S. E. Megaevolutionary dynamics and the timing of evolutionary innovation in reptiles. *Nature Communications* **11**, 3322 (2020).

66 Upham, N. S., Esselstyn, J. A. & Jetz, W. Inferring the mammal tree: species-level sets of phylogenies for questions in ecology, evolution, and conservation. *PLoS Biology* **17**, e3000494 (2019).
67 Alroy, J. The fossil record of North American mammals: evidence for a Paleocene evolutionary radiation. *Systematic Biology* **48**, 107-118 (1999).
68 Goloboff, P. A., Farris, J. S. & Nixon, K. C. TNT, a free program for phylogenetic analysis. *Cladistics* **24**, 774-786 (2008).
69 Ronquist, F. *et al.* MrBayes 3.2: efficient Bayesian phylogenetic infernece and model choice across a large model space. *Systematic Biology* **61**, 539-542 (2012).
70 Figueroa, R. T., Weinschütz, L. C. & Friedman, M. The oldest Devonian circumpolar ray-finned fish? *Biology Letters* **17**, 20200766 (2021).
71 PAUP*. Phylogenetic analysis using parsimony (*and other methods) v. 4 (Sinauer Associates, Sunderland, MA, 2003).
72 Matzke, N. J. & Wright, A. M. Inferring node dates from tip dates in fossil Canidae: the importance of tree priors. *Biology Letters* **12** (2016).
73 Revell, L. J. Two new graphical methods for mapping trait evolution of phylogenies. *Methods in Ecology and Evolution* **4**, 754-759 (2013).
74 Revell, L. J. phytools: an R package for phylogenetic comparative biology (and other things). *Methods in Ecology and Evolution* **3**, 217-223 (2012).
75 Felsenstein, J. Phylogenies and the comparative method. *The American Naturalist* **121**, 1-15 (1985).
76 Gardiner, B. G. Certain palaeoniscoid fishes and the evolution of the actinopterygian snout. *Bulletin of the British Museum (Natural History) Geology* **8**, 255-325 (1963).

A

ll
st
sorb
it
dsph
scl
op
sop
jug
mx
sc
dent
rad
br

B

mx
dmpt
ecpt
av
enpt
qu
?pmx
art
dent
t
ang
tp
part

C

scpc
clth
rad
icl
clav
lep

D

sph
?ic
unc
exo
asp
eb
psp
hmd
chy
cb

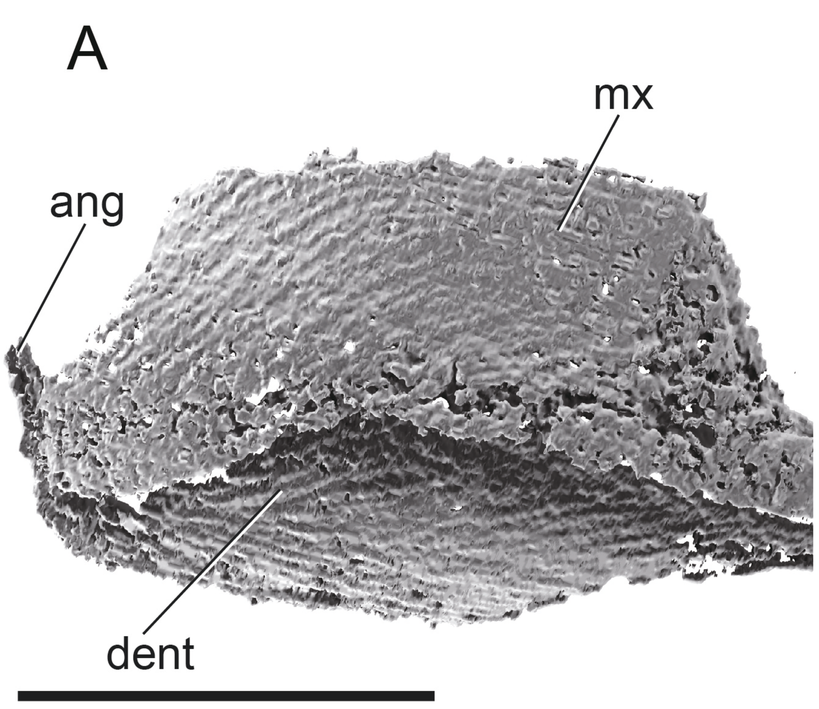
A
mx
ang
dent

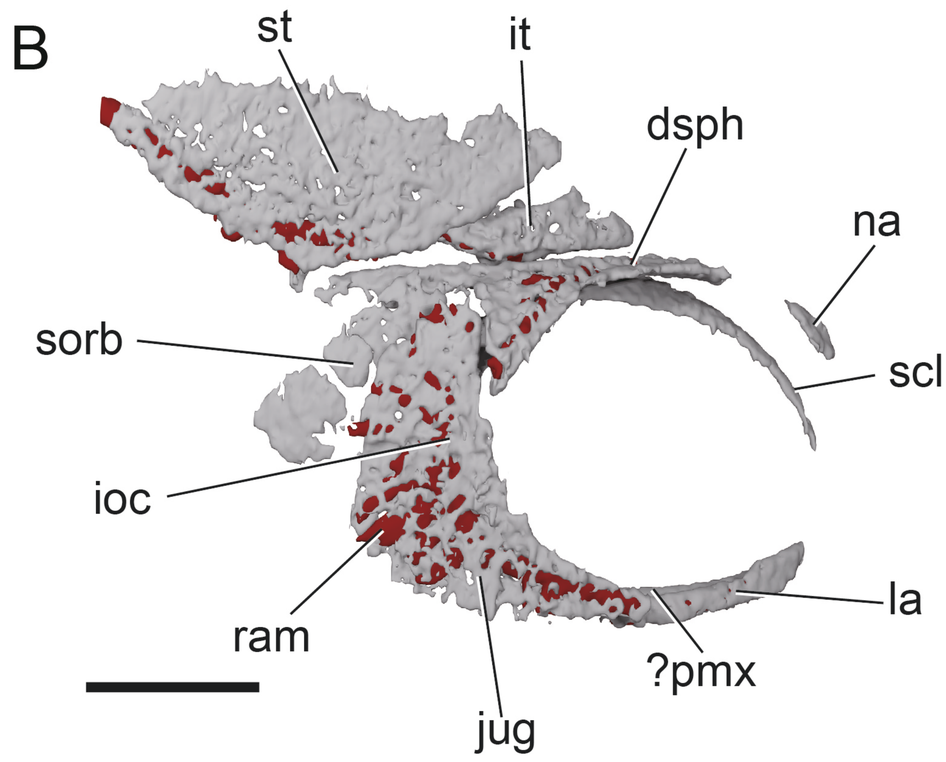
B
st
it
dsph
na
sorb
scl
ioc
la
ram
?pmx
jug

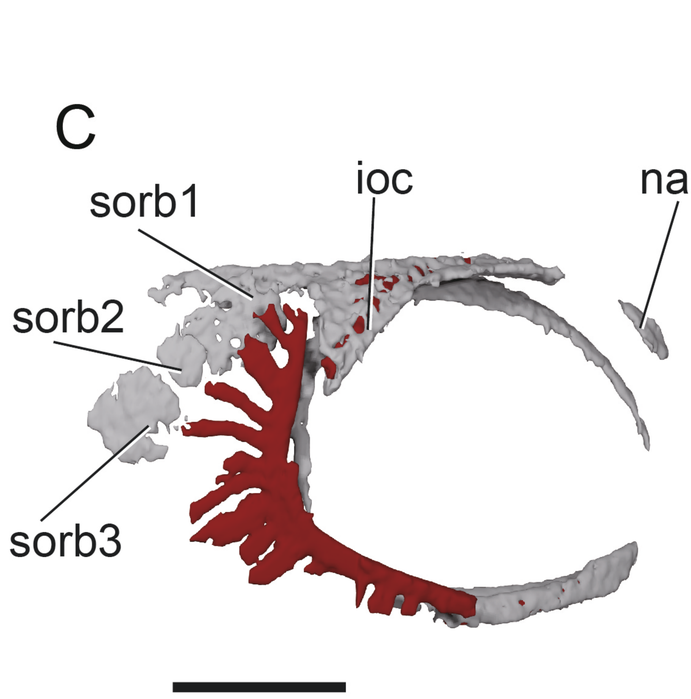
C
sorb1
ioc
na
sorb2
sorb3

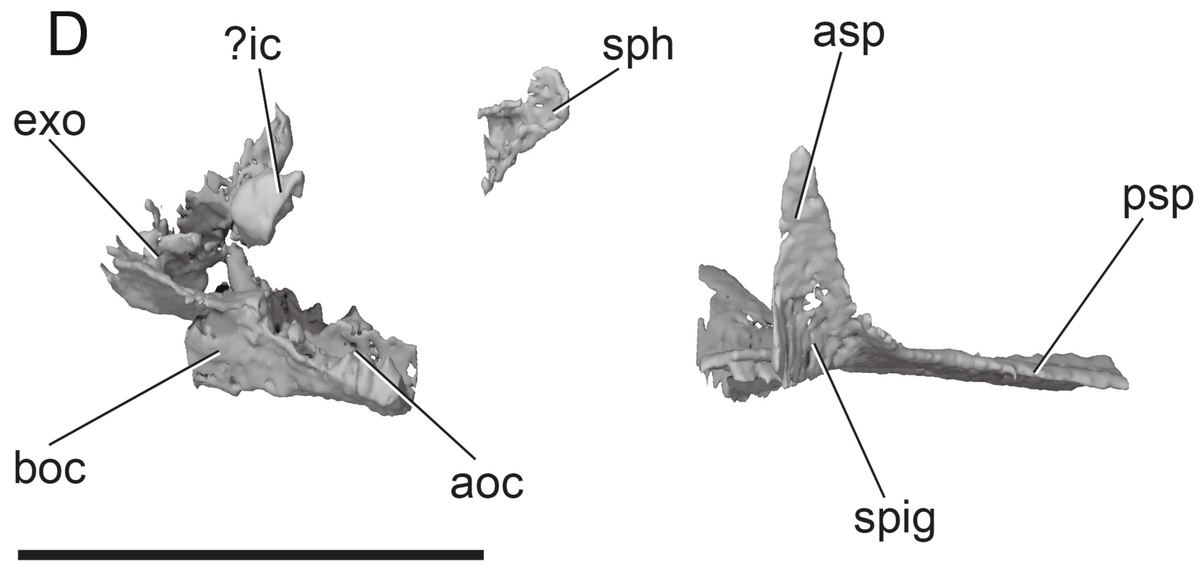
D
?ic
sph
asp
exo
psp
boc
aoc
spig

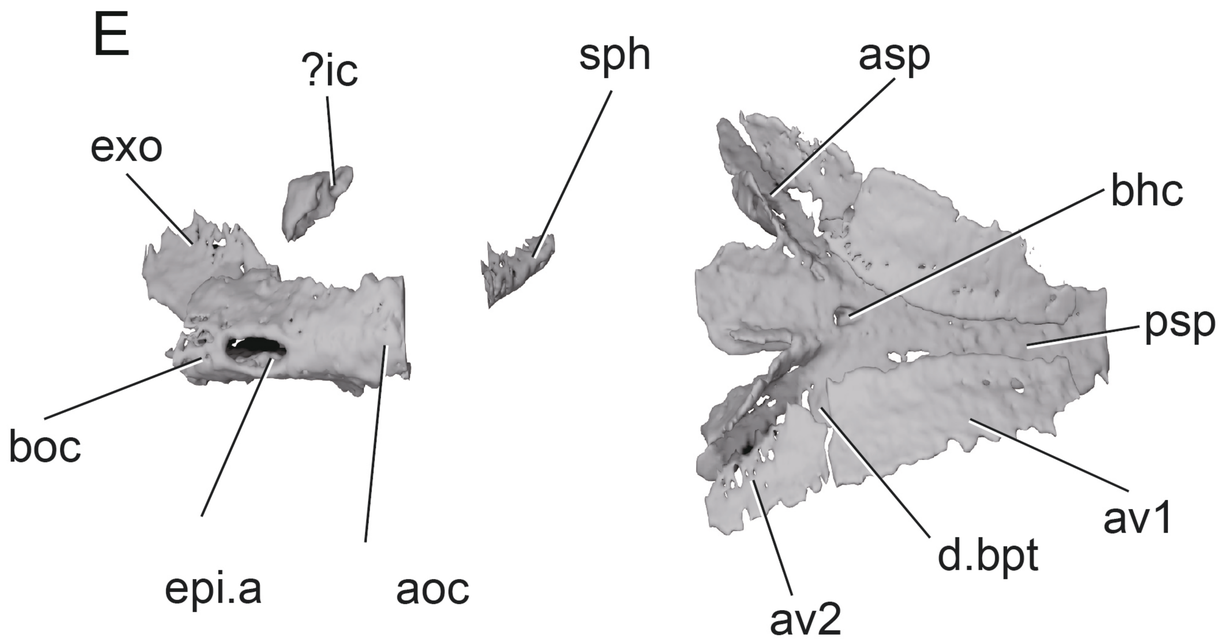
E
?ic
sph
asp
exo
bhc
psp
boc
av1
d.bpt
epi.a
aoc
av2

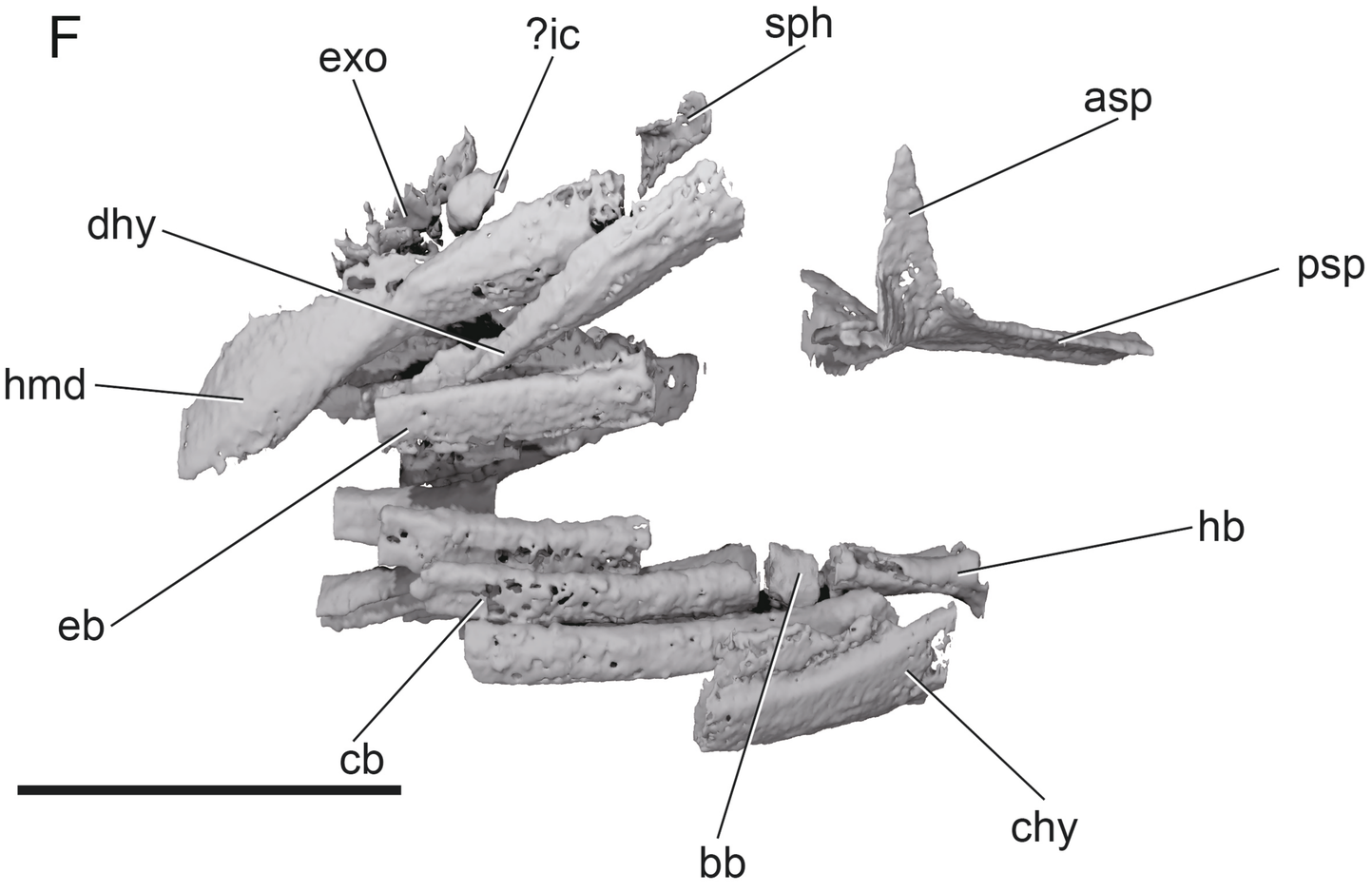
F
exo
?ic
sph
asp
dhy
psp
hmd
hb
eb
cb
bb
chy

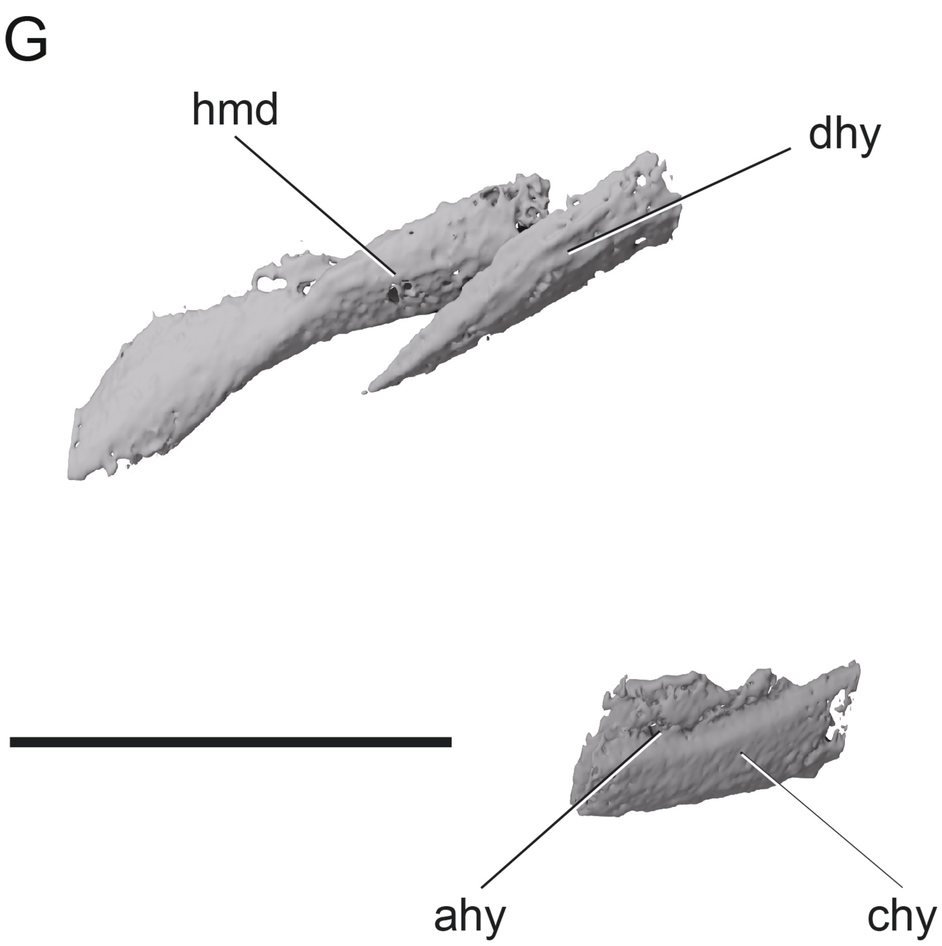
G
hmd
dhy
ahy
chy

Palaeoneiros

A

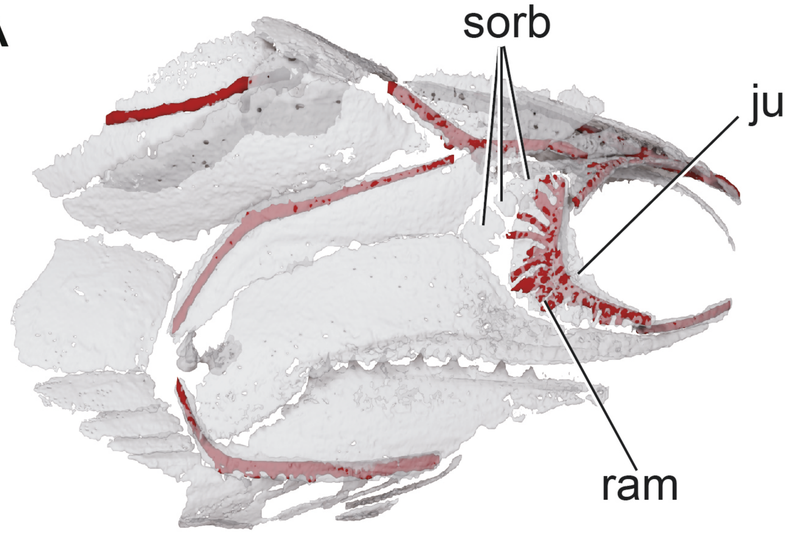

B

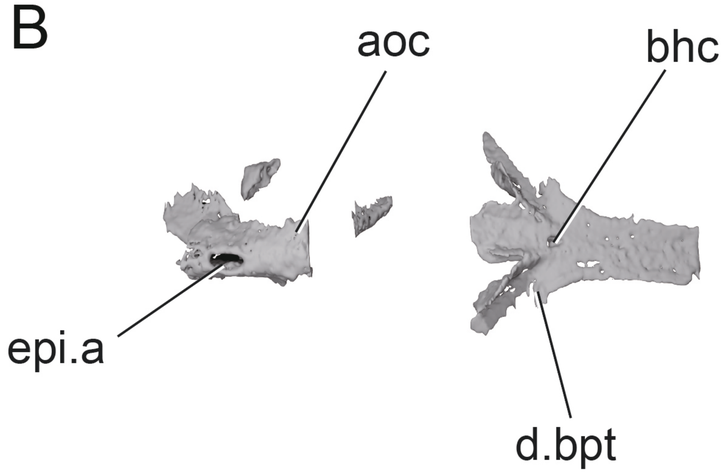

C

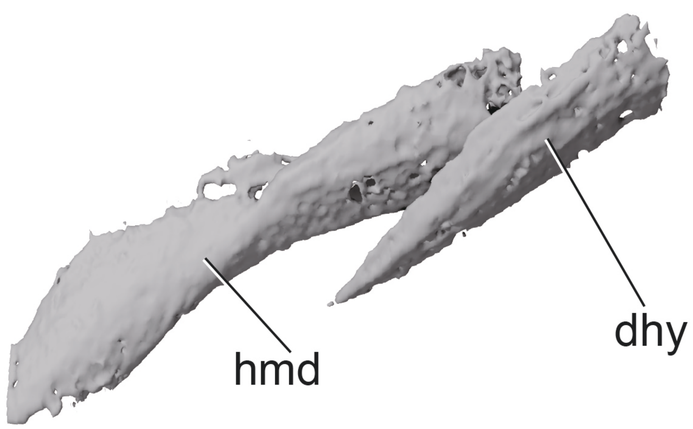

Devonian fishes

D

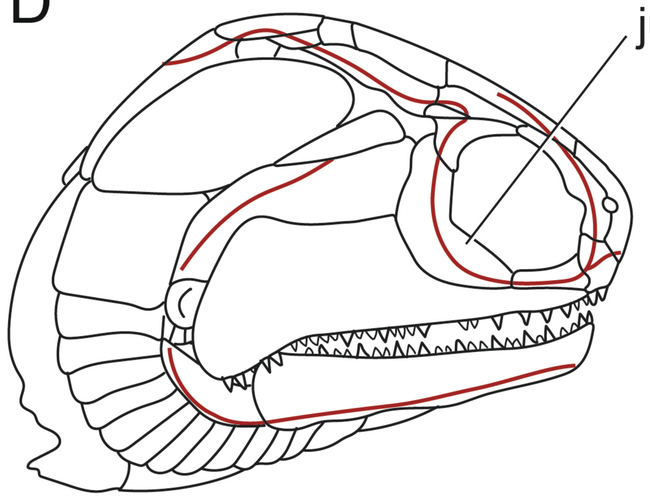

E

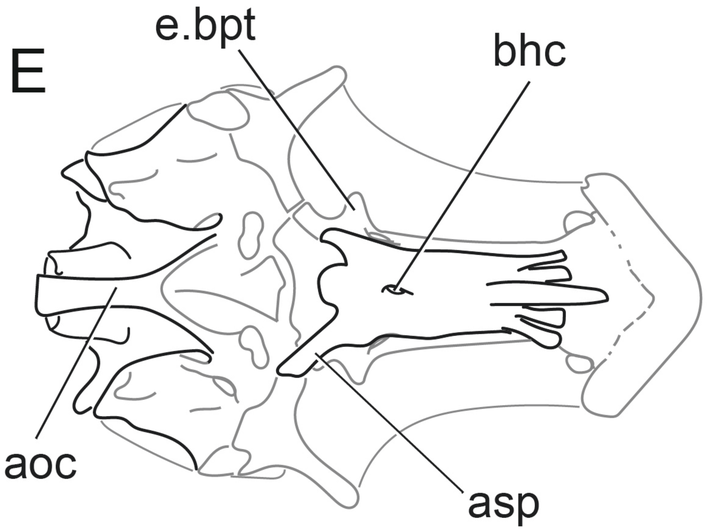

F

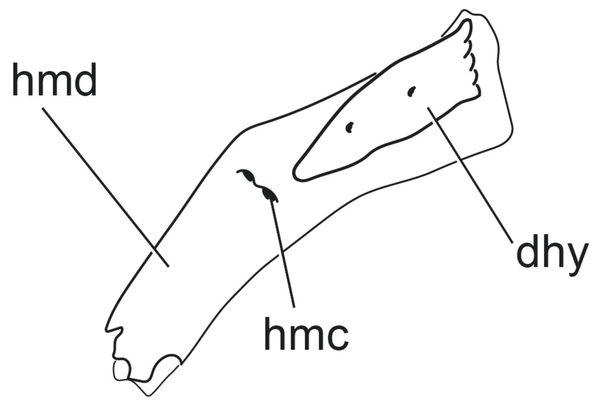

Carboniferous fishes

G

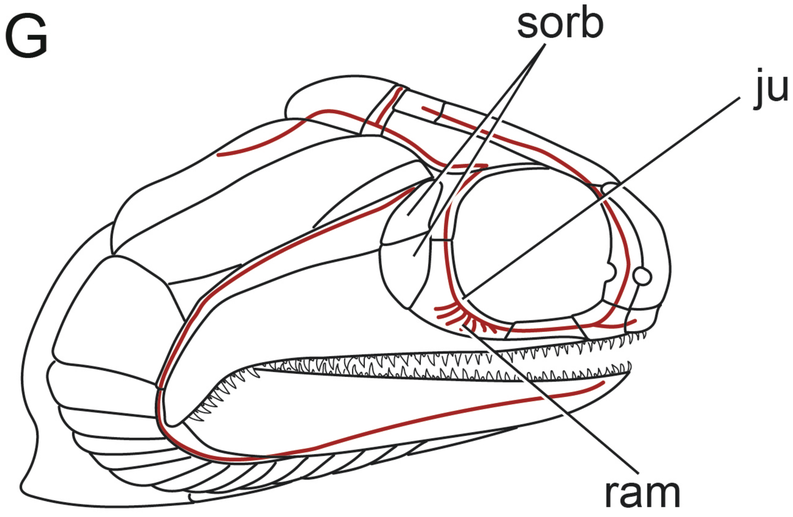

H

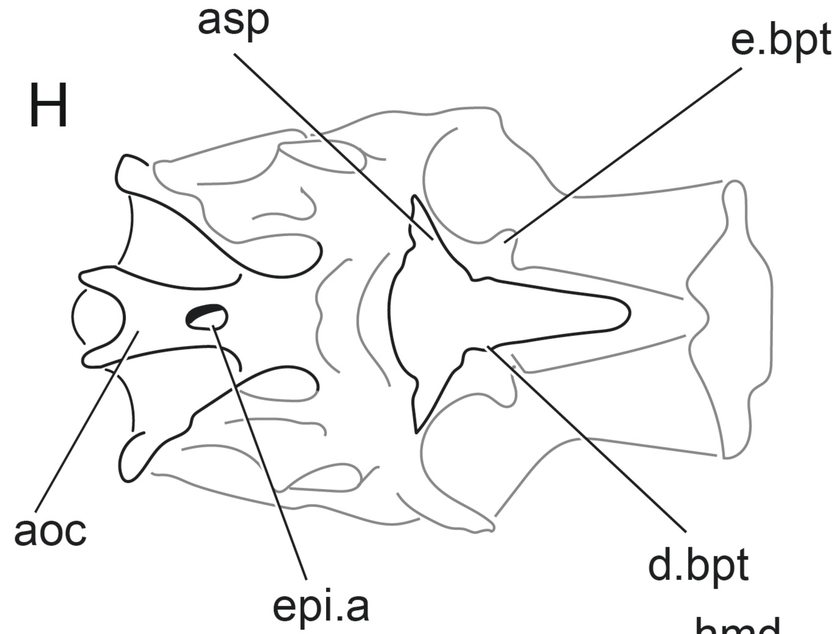

I

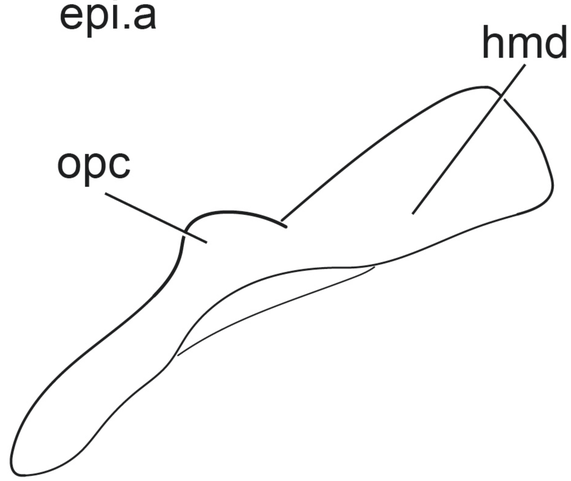

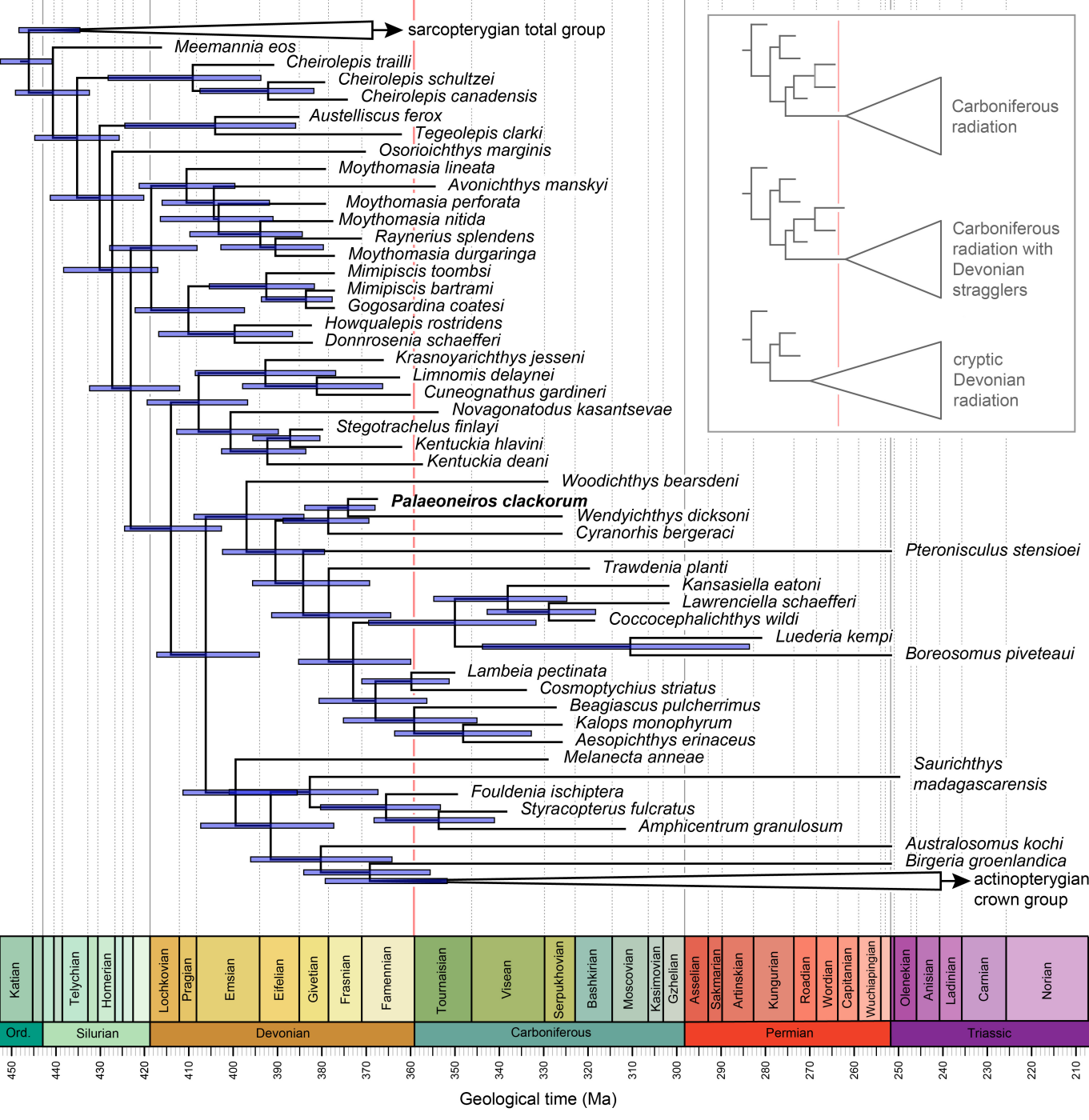
sarcopterygian total group
Meemannia eos
Cheirolepis trailli
Cheirolepis schultzei
Cheirolepis canadensis
Austelliscus ferox
Tegeolepis clarki
Osorioichthys marginis
Moythomasia lineata
Avonichthys manskyi
Moythomasia perforata
Moythomasia nitida
Raynerius splendens
Moythomasia durgaringa
Mimipiscis toombsi
Mimipiscis bartrami
Gogosardina coatesi
Howqualepis rostridens
Donnrosenia schaefferi
Krasnoyarichthys jesseni
Limnomis delaynei
Cuneognathus gardineri
Novagonatodus kasantsevae
Stegotrachelus finlayi
Kentuckia hlavini
Kentuckia deani
Woodichthys bearsdeni
Palaeoneiros clackorum
Wendyichthys dicksoni
Cyranorhis bergeraci
Pteronisculus stensioei
Trawdenia planti
Kansasiella eatoni
Lawrenciella schaefferi
Coccocephalichthys wildi
Luederia kempi
Boreosomus piveteaui
Lambeia pectinata
Cosmoptychius striatus
Beagiascus pulcherrimus
Kalops monophyrum
Aesopichthys erinaceus
Melanecta anneae
Saurichthys madagascarensis
Fouldenia ischiptera
Styracopterus fulcratus
Amphicentrum granulosum
Australosomus kochi
Birgeria groenlandica
actinopterygian crown group
Carboniferous radiation
Carboniferous radiation with Devonian stragglers
cryptic Devonian radiation
Katian
Telychian
Homerian
Lochkovian
Pragian
Emsian
Eifelian
Givetian
Frasnian
Famennian
Tournaisian
Visean
Serpukhovian
Bashkirian
Moscovian
Kasimovian
Gzhelian
Asselian
Sakmarian
Artinskian
Kungurian
Roadian
Wordian
Capitanian
Wuchiapingian
Olenekian
Anisian
Ladinian
Carnian
Norian
Ord.
Silurian
Devonian
Carboniferous
Permian
Triassic
450
440
430
420
410
400
390
380
370
360
350
340
330
320
310
300
290
280
270
260
250
240
230
220
210
Geological time (Ma)

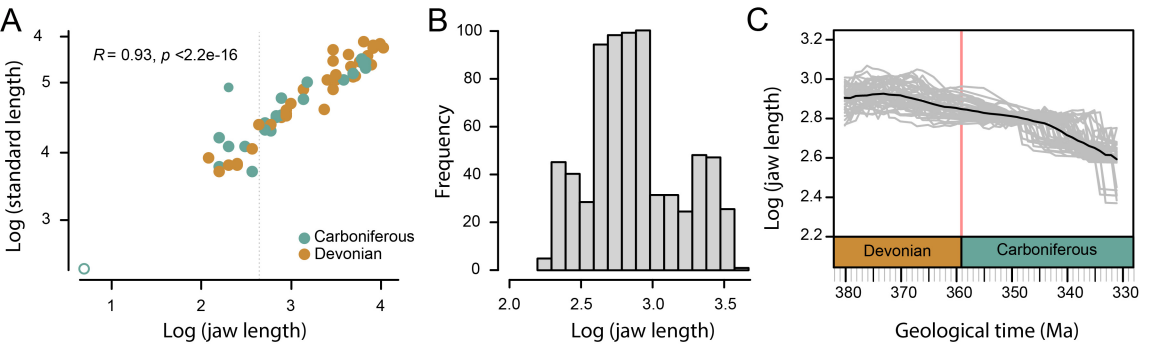
A
R = 0.93, p <2.2e-16
Carboniferous
Devonian
Log (standard length)
Log (jaw length)
B
Frequency
Log (jaw length)
C
Log (jaw length)
Devonian
Carboniferous
Geological time (Ma)

Extended Data Legends

Extended Data Fig. 1 | Geological context of *Palaeoneiros clackorum* MCZ VPF-5114. (A) Map of Pennsylvania showing location; inset shows geological map for the area of Warren County (based on (36)) and simplified geological column (based on (68)). City of Warren indicated by solid bounding lines. (B) External photograph of *Palaeoneiros clackorum* showing right lateral flank. Colors in stratigraphic column relate to geological map: latest Devonian and post-Devonian strata condensed into one color. Scale bar in (A): 10 km, in (B): 10 mm. Photo copyright President and Fellows of Harvard College.

Extended Data Fig. 2 | External photographs of *Palaeoneiros clackorum* MCZ VPF-5114. Right lateral flank in (A) part and (B) counterpart. (C) Ventral view showing entire specimen, and (D) closeup of skull and pectoral region. (E) Right anal fin. (F) Scales from right lateral flank. Scale bar in (A)-(C): 10 mm, in (D)-(F): 5 mm. Photos copyright President and Fellows of Harvard College. Abbreviations: an, anal fin; br, branchiostegal; chy, ceratohyal; clth, cleithrum; dent, dentary; dors, dorsal fin; frf, fringing fulcra; lep, lepidotrichia; mx, maxilla; pect, pectoral fin; pelv, pelvic fin; sc, scale. Photos copyright President and Fellows of Harvard College.

Extended Data Fig. 3 | Anatomy of *Palaeoneiros clackorum* MCZ VPF-5114. Interpretive drawing of (A) right lateral view of specimen; (B) medial view of right upper and lower jaws; (C) medial view of left shoulder girdle and fin, and (D) left lateral view of gill skeleton, hyoid arch and braincase. Scale bar in (A): 10 mm, in (B)-(D): 5 mm. Abbreviations: ang, angular; art, articular; asp, ascending process of parasphenoid; av, accessory vomer; br, branchiostegal; cb, ceratobranchial; chy, ceratohyal; clav, clavicle; clth, cleithrum; dent, dentary; dmpt, dermatopterygoid; dsph, dermosphenotic; ecpt, ectopterygoid and dermopalatines; eb, epibranchial; enpt, entopteryygoid; exo, exoccipital; hmd, hyomandibula; ?ic, possible intercalar; icl, interclavicle; ioc, infraorbital canal; it, intertemporal; jug, jugal; jugc, jugal canal; lep, lepidotrichia; ll, lateral line; mc, mandibular canal; mx, maxilla; op, operculum; part, prearticular and coronoid; popc, preopercular canal; popl, preopercular pit lines; ?pmx, possible premaxilla; psp, parasphenoid; qu, quadrate; rad, radials; sc, scale; scl, sclerotic ossicle; scpc, scapulocoracoid; sop, suboperculum; sorb, suborbitals; sph, sphenotic ossification; st, supratemporal; t, teeth; tp, toothplate; unc, uncinate process.

Extended Data Fig. 4 | External anatomy of *Palaeoneiros clackorum* MCZ VPF-5114. Renders of specimen in (A) right lateral, (B) left lateral, (C) dorsal, (D) anterior, and (E) ventral view; and an isolated scale (F). Colour coding of skeleton: blue, cheek and jaw; purple, skull roof and sclerotic ossicle; pink, braincase; dark green, hyomandibula; light green, operculogular system; turquoise, shoulder girdle; yellow, gill skeleton. Scale bar in (A)-(C),(E): 5 mm, in (D): 2 mm, in(F):1 mm. Abbreviations: ang, angular; antd, anterodorsal process; art, articular; asc, ascending process of the parasphenoid; av, accessory vomer; br, branchiostegal; cb, ceratobranchial; chy, ceratohyal; clav, clavicle; clth, cleithrum; dent, dentary; dsph, dermosphenotic; eb, epibranchial; ecpt, ectopterygoid and dermopalatines; enpt, entopterygoid; exsc, extrascapular; fr, frontal; fu, fused lepidotrichia; hb, hypobranchial; hmd, hyomandibula; ?ic, possible intercalar; icl, interclavicle; ioc, infraorbital canal; it, intertemporal; jgl, jugal canal; jug, jugal; lac, lacrimal; lep, lepidotrichia; ll, lateral line; mc, mandibular canal; mpl, middle pit line; mx, maxilla; op, operculum; pa, parietal; part, prearticular and coronoids; peg, scale peg; pi, pineal foramen; ?pmx, possible premaxilla; pop, preoperculum; popl, preopercular pit line; ppl, posterior pit line; pscl, presupracleithrum; psp, parasphenoid; pt, posttemporal; qu, quadrate; rad, radial; sc, scale; scl, sclerotic ossicle; sclth, supracleithrum; soc, supraorbital canal; sop, suboperculum; sorb, suborbital; sph, sphenotic ossification; st, supratemporal; unc, uncinate process. Renders copyright President and Fellows of Harvard College.

Extended Data Fig. 5 | Renders of *Palaeoneiros clackorum* MCZ VPF-5114. (A) Skull roofing bones in visceral view. (B) Possible premaxilla. (C) Right maxilla, dentary and postdentary in medial view. (D) Right lower jaw in dorsal view. (E) Left lower jaw in medial view. Scale bar in all: 2 mm. Abbreviations: add, adductor fossa; ang, angular; art, articular; dent, dentary; exsc, extrascapular; fr, frontal; ll, lateral line; mc, mandibular canal; mx, maxilla; na, nasal; ov, maxilla overlap of dentary; ?pmx, premaxilla; part, prearticular plus coronoids; pi, pineal foramen; pt, posttemporal; qu, quadrate; ri, ridge; pa, parietal; sh, maxillary shelf; soc, supraorbital canal; t, tooth; tp, toothplate. Renders copyright President and Fellows of Harvard College.

Extended Data Fig. 6 | Renders of gill skeleton of *Palaeoneiros clackorum* MCZ VPF-5114. (A) Gill skeleton in dorsal view. (B) Gill skeleton in ventral view. Scale bar: 5 mm. Abbreviations: bb, basibranchial; cb, ceratobranchial; eb, epibranchial; hb, hyobranchial; pb, pharyngobranchial. Renders copyright President and Fellows of Harvard College.

Extended Data Fig. 7 | Renders of shoulder and fin of *Palaeoneiros clackorum* MCZ VPF-5114. (A) Shoulder girdle and pectoral fin in left lateral view, and (B) closeup with dermal girdle removed. (C) Shoulder girdle and pectoral fin in medial view, and (D) with radials and lepidotrichia removed. (E) Shoulder girdle and pectoral fin in posterior view, and (F) with radials and lepidotrichia removed. Radials in (G) dorsal and (H) ventral view. Scale bar in (A)-(F): 2 mm, in (G)-(H): 1mm. Abbreviations: clav, clavicle; clth, cleithrum; fu, fused lepidotrichia; gl, glenoid fossa; icl, interclavicle; lep, lepidotrichia; mptg, metapterygium; pr.rad, preaxial radial; ptg, propterygium; ptg.ca, propterygial canal; rad, radial; scpc.hz, horizontal plate of scapulocoracoid; scpc.pl, scapulocoracoid plates. Renders copyright President and Fellows of Harvard College.

Extended Data Fig. 8 | Results of parsimony analysis. (A) Strict consensus of the 20,000 trees (1616 steps) for 121 taxa and 292 equally weighted characters. Digits above nodes indicate Bremer decay indices above 1. (B) Agreement subtree. New taxon indicated in bold.

Extended Data Fig. 9 | Results of Bayesian analysis. 50% majority rule tree for 121 taxa and 292 equally weighted characters. Digits at nodes indicate posterior probability support. New taxon indicated in bold.

Extended Data Fig. 10 | Results of fossil birth-death analysis. Blue bars associated with nodes indicate 95% highest posterior density for age estimates. New taxon indicated in bold.

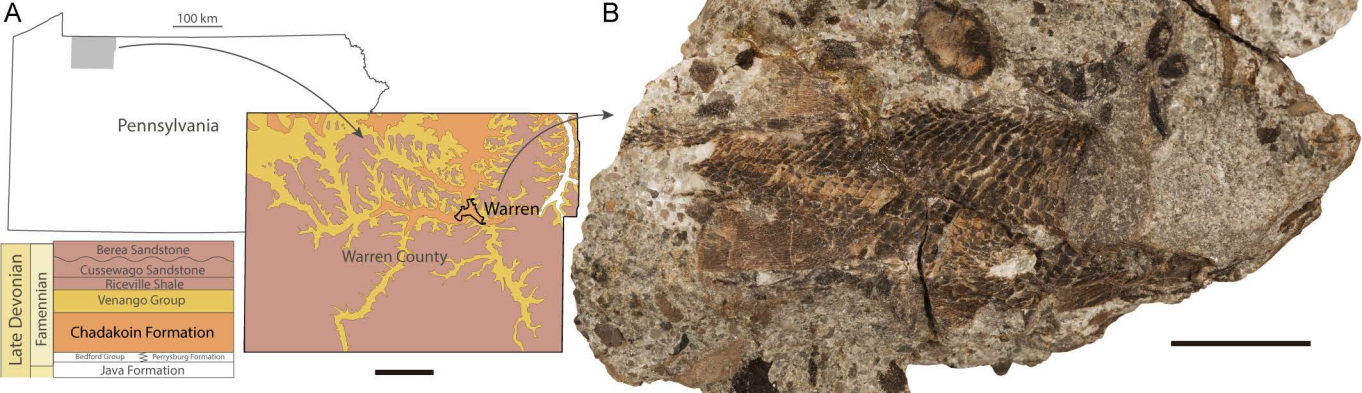
A
100 km
Pennsylvania
Warren
Warren County
Late Devonian
Famennian
Berea Sandstone
Cussewago Sandstone
Riceville Shale
Venango Group
Chadakoin Formation
Bedford Group
Perrysburg Formation
Java Formation
B

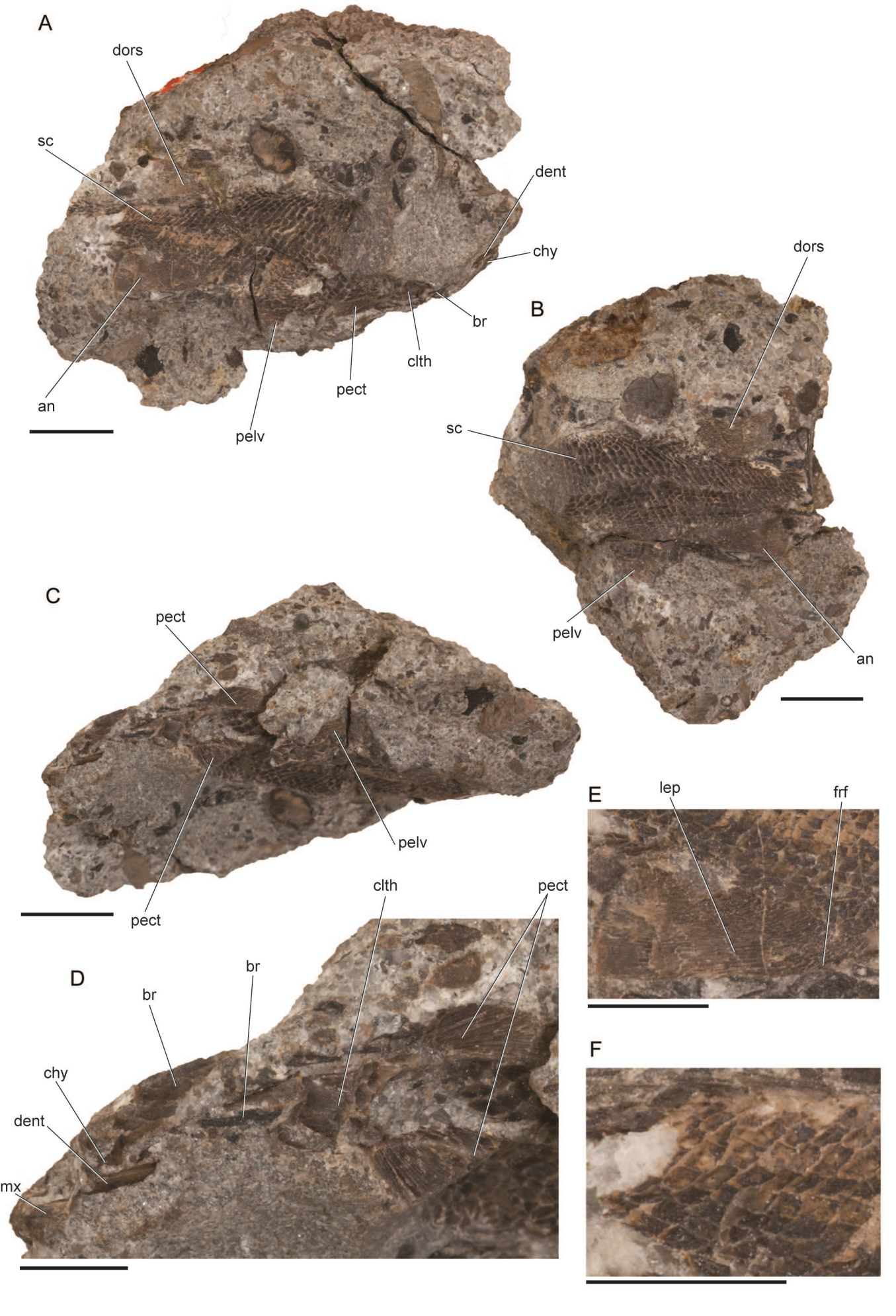
A
dors
sc
dent
chy
br
clth
pect
pelv
an
B
dors
sc
pelv
an
C
pect
pelv
pect
D
clth
pect
br
br
chy
dent
mx
E
lep
frf
F

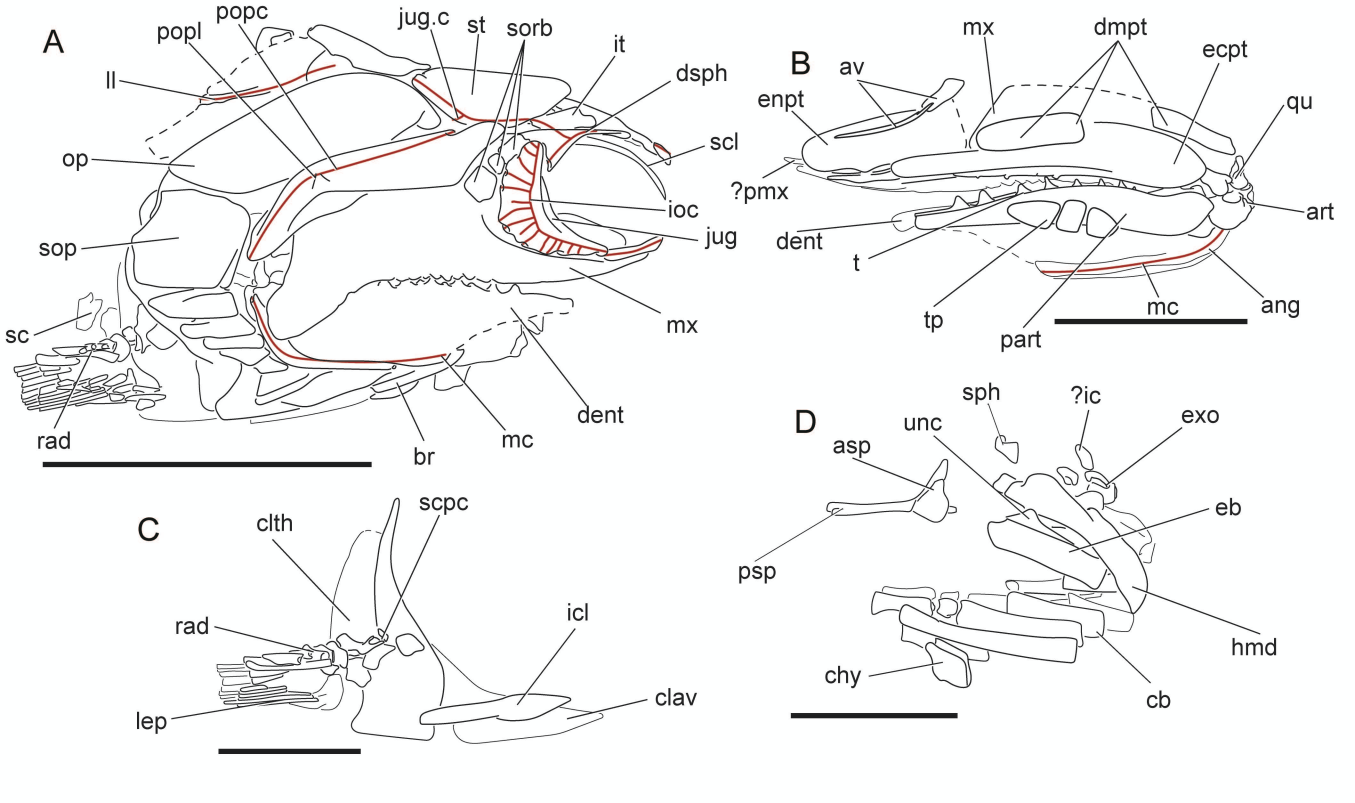
A
popl
popc
jug.c
st
sorb
it
dsph
ll
scl
op
ioc
jug
sop
mx
sc
dent
rad
br
mc
B
mx
dmpt
ecpt
av
enpt
qu
?pmx
art
dent
t
tp
part
mc
ang
C
clth
scpc
rad
icl
lep
clav
D
sph
?ic
exo
unc
asp
eb
psp
hmd
chy
cb

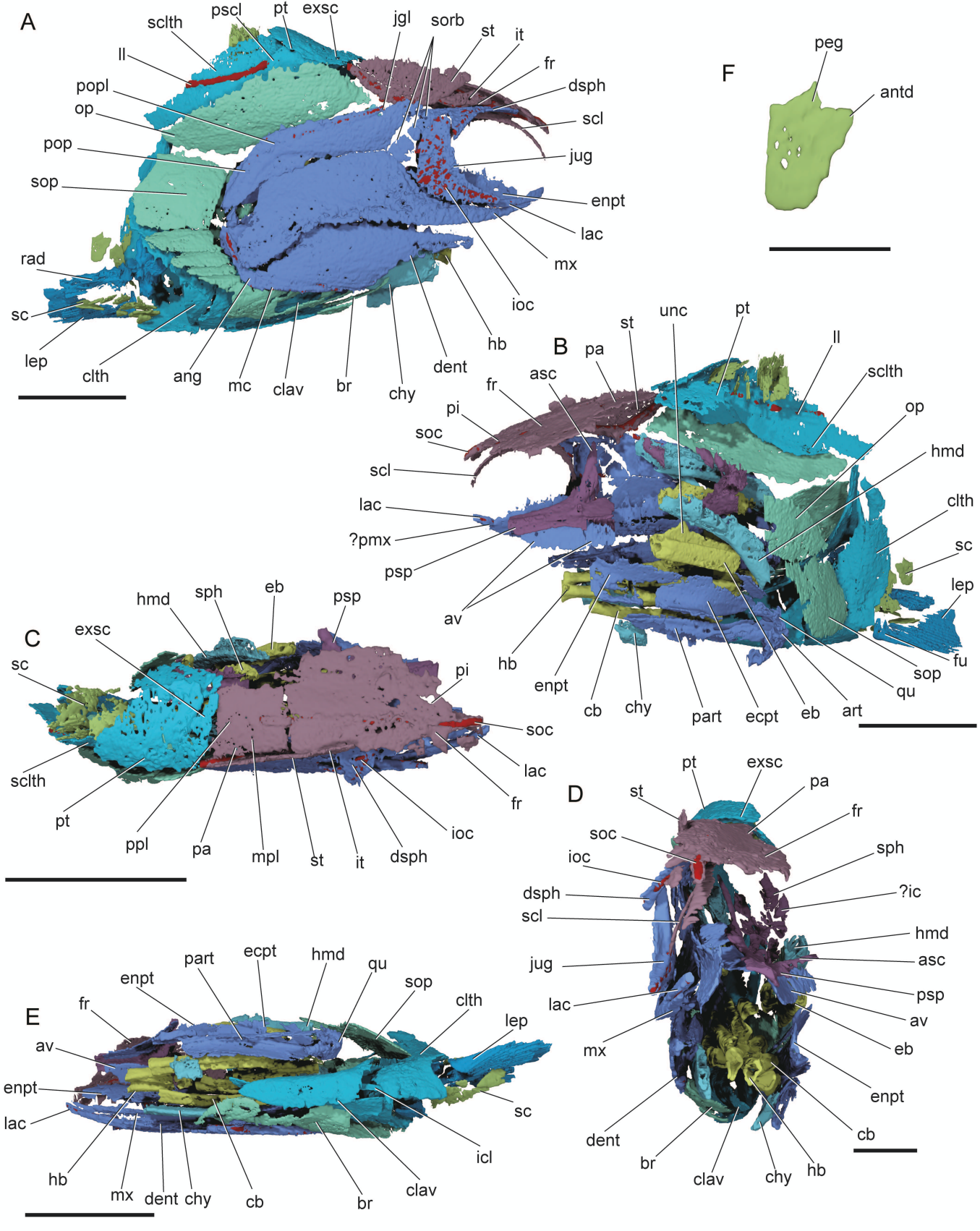
A
sclth
pscl
pt
exsc
jgl
sorb
st
it
ll
fr
popl
dsph
op
scl
pop
jug
sop
enpt
lac
mx
rad
ioc
sc
hb
lep
clth
ang
mc
clav
br
chy
dent
F
peg
antd
B
pa
st
unc
pt
ll
asc
sclth
fr
op
pi
hmd
soc
scl
clth
lac
sc
?pmx
psp
lep
av
fu
sop
hb
qu
enpt
cb
chy
part
ecpt
eb
art
C
hmd
sph
eb
psp
exsc
sc
pi
soc
lac
sclth
fr
pt
ioc
ppl
pa
mpl
st
it
dsph
D
pt
exsc
pa
st
fr
soc
sph
ioc
?ic
dsph
scl
hmd
jug
asc
psp
lac
av
mx
eb
enpt
cb
dent
br
clav
chy
hb
E
part
ecpt
hmd
qu
sop
enpt
fr
clth
lep
av
enpt
sc
lac
icl
hb
mx
dent
chy
cb
br
clav

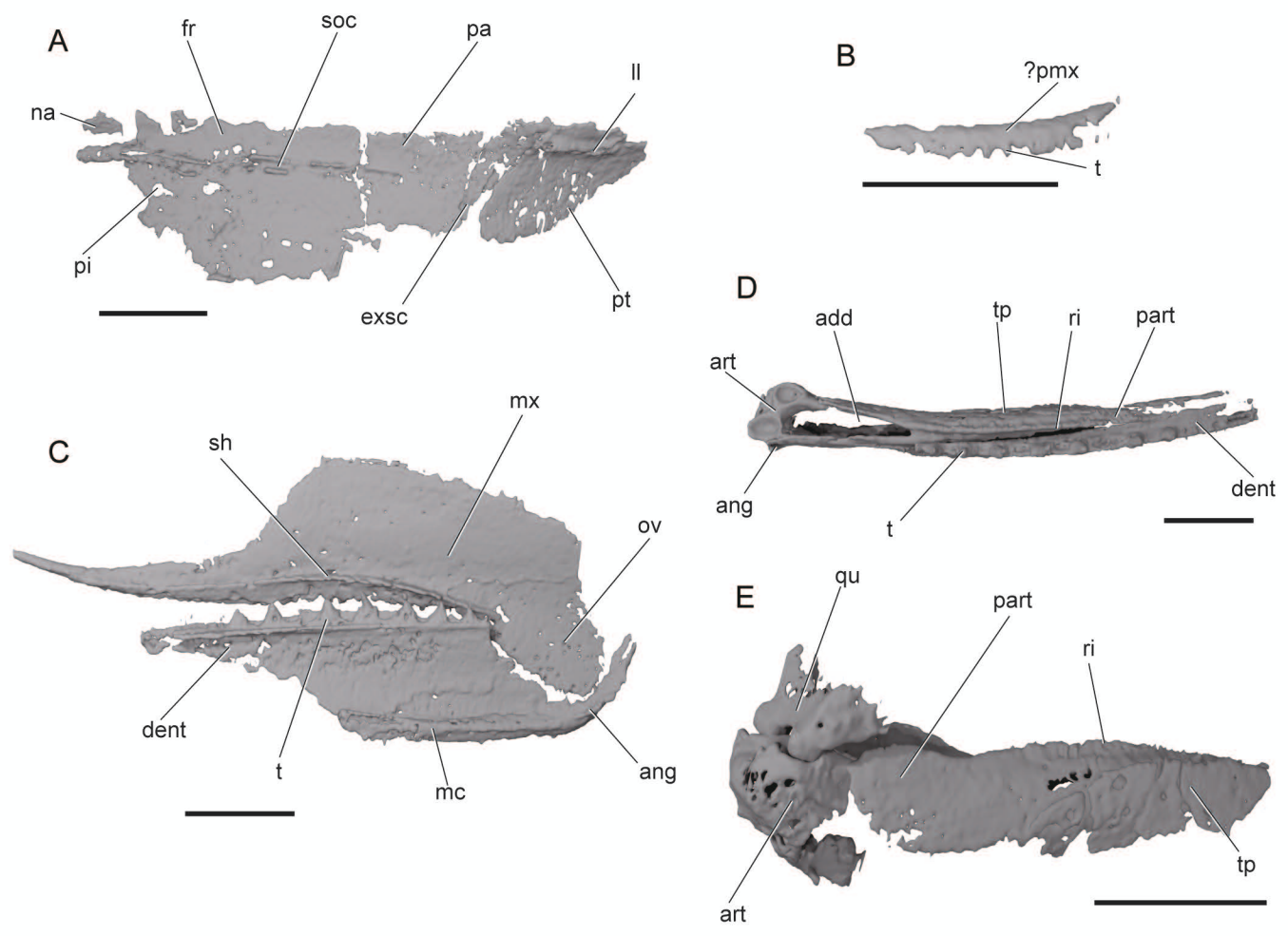
A
fr
soc
pa
ll
na
pi
exsc
pt
B
?pmx
t
C
sh
mx
ov
dent
t
mc
ang
D
add
tp
ri
part
art
ang
t
dent
E
qu
part
ri
art
tp

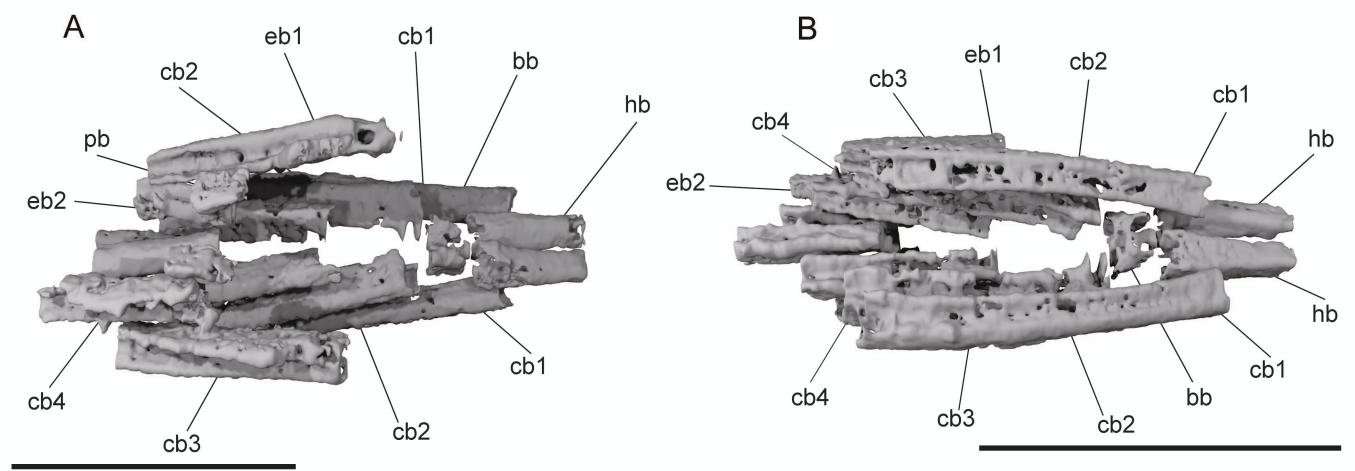
A
eb1
cb1
cb2
bb
hb
pb
eb2
cb1
cb4
cb3
cb2
B
cb3
eb1
cb2
cb1
cb4
hb
eb2
hb
cb1
cb4
bb
cb3
cb2

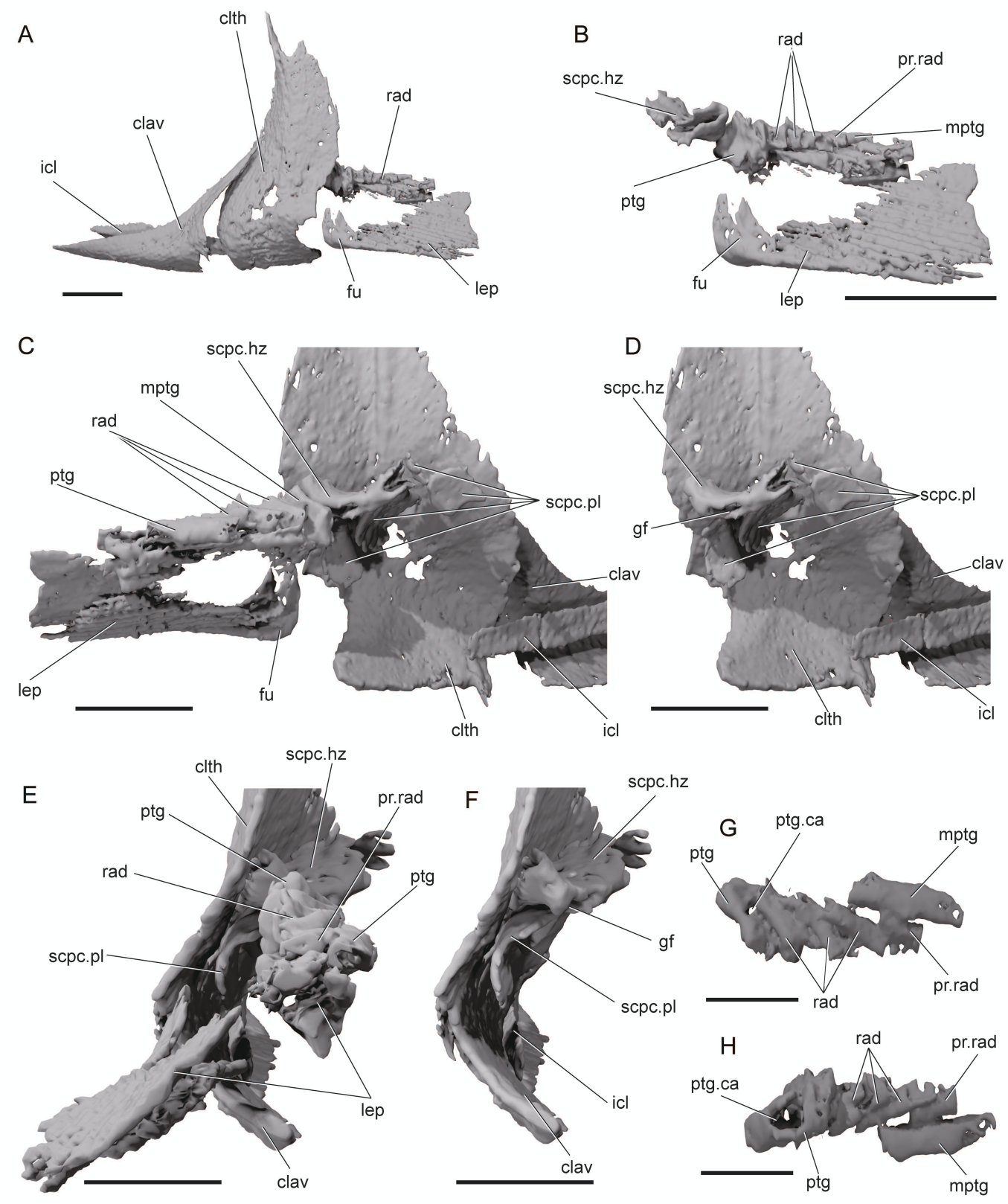
A
clth
clav
rad
icl
fu
lep
B
rad
pr.rad
scpc.hz
mptg
ptg
fu
lep
C
scpc.hz
mptg
rad
ptg
scpc.pl
clav
lep
fu
clth
icl
D
scpc.hz
scpc.pl
gf
clav
clth
icl
E
clth
scpc.hz
pr.rad
ptg
rad
ptg
scpc.pl
lep
clav
F
scpc.hz
gf
scpc.pl
icl
clav
G
ptg.ca
mptg
ptg
pr.rad
rad
H
rad
pr.rad
ptg.ca
ptg
mptg


A
Dicksonosteus arcticus
Entelognathus primordialis
Acanthodes bronni
Cladodoides wildungensis
Ozarcus mapesae
Dialipina salguerioensis
'Ligulalepis'
Onychodus jandemarrai
Guiyu oneiros
Psarolepis romeri
Styloichthys changae
Diplocercides kayseri
Miguashaia bureaui
Glyptolepis groenlandica
Porolepis sp.
Gogonasus andrewsae
Eusthenopteron foordi
Osteolepis macrolepidotus
Meemannia eos
Cheirolepis trailli
Cheirolepis canadensis
Cheirolepis schultzei
Tegeolepis clarki
Austelliscus ferox
Osorioichthys marginis
Raynerius splendens
Moythomasia durgaringa
Moythomasia nitida
Moythomasia perforata
Moythomasia lineata
Avonichthys manskyi
Donnrosenia schaefferi
Howqualepis rostridens
Mimipiscis toombsi
Gogosardina coatesi
Mimipiscis bartrami
Krasnoyarichthys jesseni
Cuneognathus gardineri
Limnomis delayni
Novagonatodus kasantsevae
Kentuckia deani
Kentuckia hlavini
Stegotrachelus finlayi
Melanecta anneae
Woodichthys bearsdeni
Cyranorhis bergeraci
Wendyichthys dicksoni
Palaeoneiros clackorum
Pteronisculus stensioi
Trawdenia planti
Cosmoptychius striatus
Lambeia pectinata
Beagiascus pulcherrimus
Aesopichthys erinaceus
Kalops monophyrum
Boreosomus piveteaui
Luederia kempi
Kansasiella eatoni
Coccocephalichthys wildi
Lawrenciella schaefferi
Saurichthys madagascarensis
Amphicentrum granulosum
Fouldenia ischiptera
Styracopterus fulcratus
Australosomus kochi
Birgeria groenlandica
Platysomus superbus
Acipenser brevirostrum
Chondrosteus acipenseroides
Erpetoichthys calabaricus
Polypterus bichir
Tanaocrossus kalliokoskii
Evenkia eunoptera
Beishanichthys brevicaudalis
Fukangichthys longidorsalis
Scanilepis dubia
Luganoia lepidosteoides
Dipteronotus ornatus
Peltopleurus lissocephalus
Discoserra pectinodon
Bobosatrania groenlandica
Ebenaqua ritchei
Gibbodon cenensis
Brembodus ridens
Eomesodon liassicus
Mesturus sp.
Arduafrons prominoris
Mesturus verrucosus
Venusichthys comptus
Dorsetichthys bechei
Leptolepis bronni
Ichthyokentema purbeckensis
Elops hawaiensis
Hiodon alosoides
Hulettia americana
Macrepistius arenatus
Watsonulus eugnathoides
Amia calva
Caturus furcatus
Obaichthys decoratus
Atractosteus spatula
Lepisosteus osseus
Macrosemimimus lennieri
Semionotus elegans
Macrosemius rostratus
Propterus elongatus
Tetragonolepis semicincta
Tetragonolepis oldhami
Aetholepis mirabilis
Heterostrophus phillipsi
Dapedium stollorum
Dapedium sp. (Lias)
Dapedium pholidotum
Dapedium caelatum
Scopulipiscis saxciput
Dapedium punctatum
Paradapedium egertoni
Hemicalypterus weiri
Dapedium noricum
Sargodon tomicus
Dandya ovalis
B
Dicksonosteus arcticus
Entelognathus primordialis
Acanthodes bronni
Cladodoides wildungensis
Ozarcus mapesae
Dialipina salguerioensis
'Ligulalepis'
Styloichthys changae
Diplocercides kayseri
Miguashaia bureaui
Glyptolepis groenlandica
Porolepis sp.
Gogonasus andrewsae
Eusthenopteron foordi
Osteolepis macrolepidotus
Cheirolepis trailli
Cheirolepis canadensis
Cheirolepis schultzei
Tegeolepis clarki
Austelliscus ferox
Osorioichthys marginis
Moythomasia lineata
Donnrosenia schaefferi
Howqualepis rostridens
Mimipiscis toombsi
Gogosardina coatesi
Mimipiscis bartrami
Raynerius splendens
Moythomasia durgaringa
Moythomasia nitida
Krasnoyarichthys jesseni
Cuneognathus gardineri
Limnomis delayni
Novagonatodus kasantsevae
Kentuckia deani
Kentuckia hlavini
Stegotrachelus finlayi
Woodichthys bearsdeni
Cyranorhis bergeraci
Wendyichthys dicksoni
Palaeoneiros clackorum
Pteronisculus stensioi
Trawdenia planti
Cosmoptychius striatus
Lambeia pectinata
Beagiascus pulcherrimus
Aesopichthys erinaceus
Kalops monophyrum
Boreosomus piveteaui
Luederia kempi
Kansasiella eatoni
Coccocephalichthys wildi
Lawrenciella schaefferi
Amphicentrum granulosum
Fouldenia ischiptera
Australosomus kochi
Birgeria groenlandica
Platysomus superbus
Acipenser brevirostrum
Chondrosteus acipenseroides
Erpetoichthys calabaricus
Polypterus bichir
Tanaocrossus kalliokoskii
Evenkia eunoptera
Beishanichthys brevicaudalis
Fukangichthys longidorsalis
Scanilepis dubia
Discoserra pectinodon
Bobosatrania groenlandica
Ebenaqua ritchei
Gibbodon cenensis
Brembodus ridens
Eomesodon liassicus
Arduafrons prominoris
Mesturus verrucosus
Venusichthys comptus
Dorsetichthys bechei
Leptolepis bronni
Ichthyokentema purbeckensis
Elops hawaiensis
Hiodon alosoides
Tetragonolepis semicincta
Tetragonolepis oldhami
Heterostrophus phillipsi
Dapedium punctatum
Dapedium sp. (Lias)
Dapedium pholidotum
Paradapedium egertoni
Hemicalypterus weiri
Dapedium noricum
Sargodon tomicus
Hulettia americana
Macrepistius arenatus
Watsonulus eugnathoides
Amia calva
Caturus furcatus
Obaichthys decoratus
Atractosteus spatula
Lepisosteus osseus
Macrosemimimus lennieri
Semionotus elegans
Macrosemius rostratus
Propterus elongatus

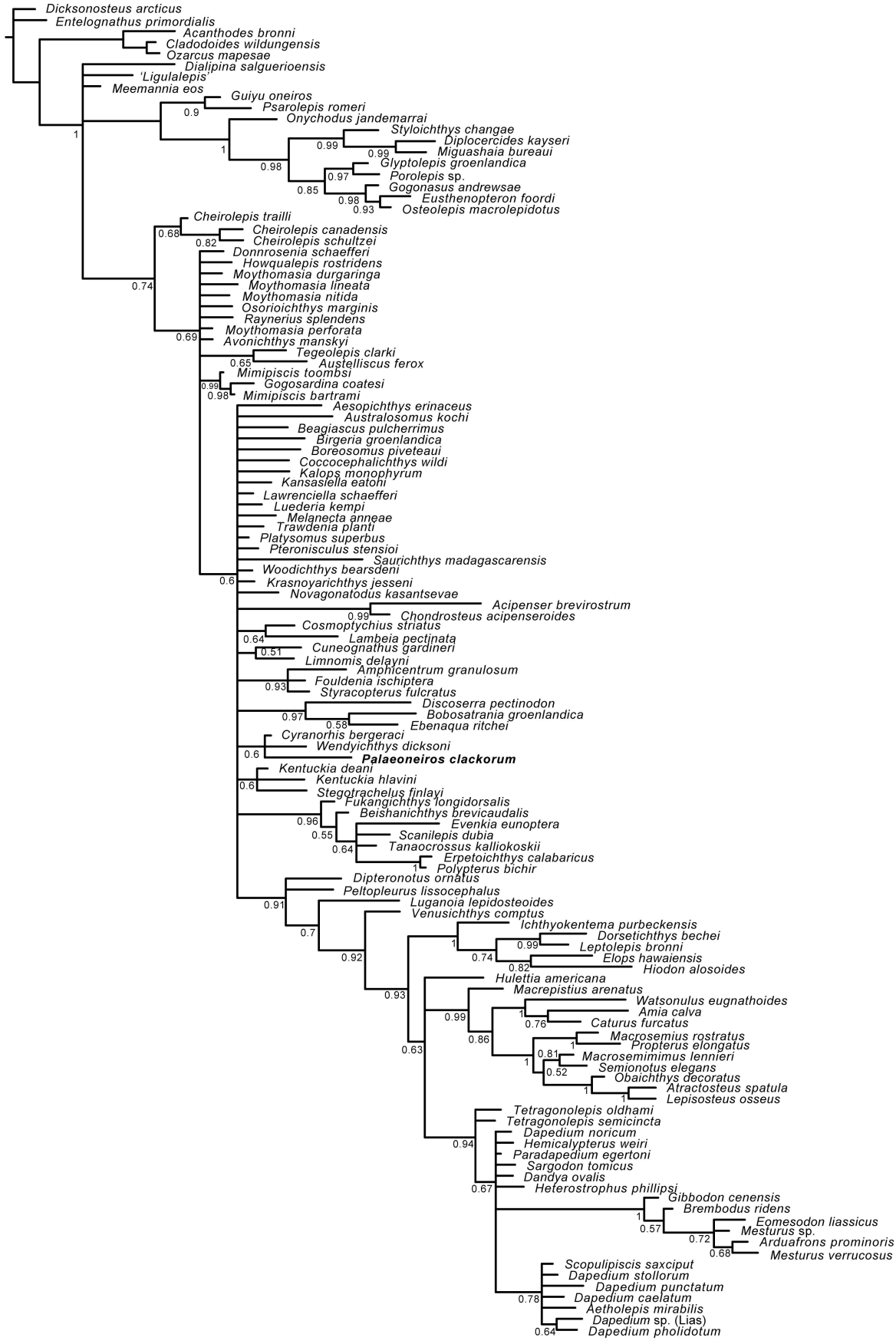
Dicksonosteus arcticus
Entelognathus primordialis
Acanthodes bronni
Cladodoides wildungensis
Ozarcus mapesae
Dialipina salguerioensis
'Ligulalepis'
Meemannia eos
Guiyu oneiros
Psarolepis romeri
Onychodus jandemarrai
Styloichthys changae
Diplocercides kayseri
Miguashaia bureaui
Glyptolepis groenlandica
Porolepis sp.
Gogonasus andrewsae
Eusthenopteron foordi
Osteolepis macrolepidotus
Cheirolepis trailli
Cheirolepis canadensis
Cheirolepis schultzei
Donnrosenia schaefferi
Howqualepis rostridens
Moythomasia durgaringa
Moythomasia lineata
Moythomasia nitida
Osorioichthys marginis
Raynerius splendens
Moythomasia perforata
Avonichthys manskyi
Tegeolepis clarki
Austelliscus ferox
Mimipiscis toombsi
Gogosardina coatesi
Mimipiscis bartrami
Aesopichthys erinaceus
Australosomus kochi
Beagiascus pulcherrimus
Birgeria groenlandica
Boreosomus piveteaui
Coccocephalichthys wildi
Kalops monophyrum
Kansaslella eatoni
Lawrenciella schaefferi
Luederia kempi
Melanecta anneae
Trawdenia planti
Platysomus superbus
Pteronisculus stensioi
Saurichthys madagascarensis
Woodichthys bearsdeni
Krasnoyarichthys jesseni
Novagonatodus kasantsevae
Acipenser brevirostrum
Chondrosteus acipenseroides
Cosmoptychius striatus
Lambeia pectinata
Cuneognathus gardineri
Limnomis delayni
Amphicentrum granulosum
Fouldenia ischiptera
Styracopterus fulcratus
Discoserra pectinodon
Bobosatrania groenlandica
Ebenaqua ritchei
Cyranorhis bergeraci
Wendyichthys dicksoni
Palaeoneiros clackorum
Kentuckia deani
Kentuckia hlavini
Stegotrachelus finlayi
Fukangichthys longidorsalis
Beishanichthys brevicaudalis
Evenkia eunoptera
Scanilepis dubia
Tanaocrossus kalliokoskii
Erpetoichthys calabaricus
Polypterus bichir
Dipteronotus ornatus
Peltopleurus lissocephalus
Luganoia lepidosteoides
Venusichthys comptus
Ichthyokentema purbeckensis
Dorsetichthys bechei
Leptolepis bronni
Elops hawaiensis
Hiodon alosoides
Hulettia americana
Macrepistius arenatus
Watsonulus eugnathoides
Amia calva
Caturus furcatus
Macrosemius rostratus
Propterus elongatus
Macrosemimimus lennieri
Semionotus elegans
Obaichthys decoratus
Atractosteus spatula
Lepisosteus osseus
Tetragonolepis oldhami
Tetragonolepis semicincta
Dapedium noricum
Hemicalypterus weiri
Paradapedium egertoni
Sargodon tomicus
Dandya ovalis
Heterostrophus phillipsi
Gibbodon cenensis
Brembodus ridens
Eomesodon liassicus
Mesturus sp.
Arduafrons prominoris
Mesturus verrucosus
Scopulipiscis saxciput
Dapedium stollorum
Dapedium punctatum
Dapedium caelatum
Aetholepis mirabilis
Dapedium sp. (Lias)
Dapedium pholidotum

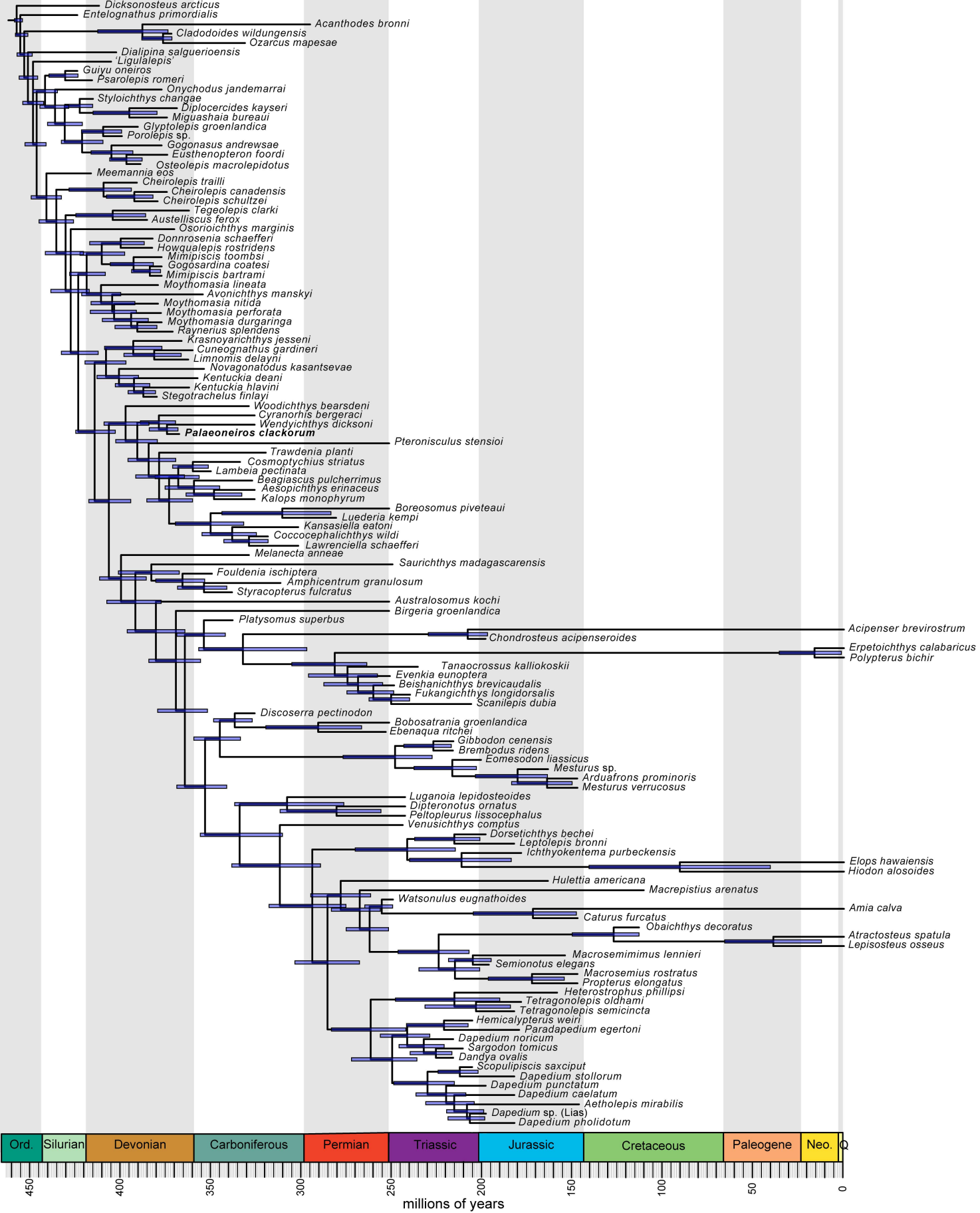
Dicksonosteus arcticus
Entelognathus primordialis
Acanthodes bronni
Cladodoides wildungensis
Ozarcus mapesae
Dialipina salguerioensis
'Ligulalepis'
Guiyu oneiros
Psarolepis romeri
Onychodus jandemarrai
Styloichthys changae
Diplocercides kayseri
Miguashaia bureaui
Glyptolepis groenlandica
Porolepis sp.
Gogonasus andrewsae
Eusthenopteron foordi
Osteolepis macrolepidotus
Meemannia eos
Cheirolepis trailli
Cheirolepis canadensis
Cheirolepis schultzei
Tegeolepis clarki
Austelliscus ferox
Osorioichthys marginis
Donnrosenia schaefferi
Howqualepis rostridens
Mimipiscis toombsi
Gogosardina coatesi
Mimipiscis bartrami
Moythomasia lineata
Avonichthys manskyi
Moythomasia nitida
Moythomasia perforata
Moythomasia durgaringa
Raynerius splendens
Krasnoyarichthys jesseni
Cuneognathus gardineri
Limnomis delayni
Novagonatodus kasantsevae
Kentuckia deani
Kentuckia hlavini
Stegotrachelus finlayi
Woodichthys bearsdeni
Cyranorhis bergeraci
Wendyichthys dicksoni
Palaeoneiros clackorum
Pteronisculus stensioi
Trawdenia planti
Cosmoptychius striatus
Lambeia pectinata
Beagiascus pulcherrimus
Aesopichthys erinaceus
Kalops monophyrum
Boreosomus piveteaui
Luederia kempi
Kansasiella eatoni
Coccocephalichthys wildi
Lawrenciella schaefferi
Melanecta anneae
Saurichthys madagascarensis
Fouldenia ischiptera
Amphicentrum granulosum
Styracopterus fulcratus
Australosomus kochi
Birgeria groenlandica
Platysomus superbus
Acipenser brevirostrum
Chondrosteus acipenseroides
Erpetoichthys calabaricus
Polypterus bichir
Tanaocrossus kalliokoskii
Evenkia eunoptera
Beishanichthys brevicaudalis
Fukangichthys longidorsalis
Scanilepis dubia
Discoserra pectinodon
Bobosatrania groenlandica
Ebenaqua ritchei
Gibbodon cenensis
Brembodus ridens
Eomesodon liassicus
Mesturus sp.
Arduafrons prominoris
Mesturus verrucosus
Luganoia lepidosteoides
Dipteronotus ornatus
Peltopleurus lissocephalus
Venusichthys comptus
Dorsetichthys bechei
Leptolepis bronni
Ichthyokentema purbeckensis
Elops hawaiensis
Hiodon alosoides
Hulettia americana
Macrepistius arenatus
Watsonulus eugnathoides
Amia calva
Caturus furcatus
Obaichthys decoratus
Atractosteus spatula
Lepisosteus osseus
Macrosemimimus lennieri
Semionotus elegans
Macrosemius rostratus
Propterus elongatus
Heterostrophus phillipsi
Tetragonolepis oldhami
Tetragonolepis semicincta
Hemicalypterus weiri
Paradapedium egertoni
Dapedium noricum
Sargodon tomicus
Dandya ovalis
Scopulipiscis saxciput
Dapedium stollorum
Dapedium punctatum
Dapedium caelatum
Aetholepis mirabilis
Dapedium sp. (Lias)
Dapedium pholidotum
Ord.
Silurian
Devonian
Carboniferous
Permian
Triassic
Jurassic
Cretaceous
Paleogene
Neo.
Q
450
400
350
300
250
200
150
100
50
0
millions of years